

**SIMULATION OF STEAM  
PRESSURIZING TANK TRANSIENTS  
BY ANALOG COMPUTER**

---

**Donald Britton Bosley  
and  
Roth S. Leddick**

Library  
U. S. Naval Postgraduate School  
Monterey, California









SIMULATION OF STEAM  
PRESSURIZING TANK TRANSIENTS  
BY ANALOG COMPUTER

\* \* \* \* \*

Donald B. Bosley

Roth S. Leddick





8854

BOSLEY

1956

THESIS  
B725

Letter on cover:

SIMULATION OF STEAM PRESSURIZING  
TANK TRANSIENTS BY ANALOG  
COMPUTER

Donald Eritton Bosley



SIMULATION OF STEAM  
PRESSURIZING TANK TRANSIENTS  
BY ANALOG COMPUTER

BY

Donald Britton Bosley  
Lieutenant, United States Navy

AND

Roth Sumner Leddick  
Lieutenant, United States Navy

Submitted in partial fulfillment  
of the requirements  
for the degree of  
MASTER OF SCIENCE  
IN  
MECHANICAL ENGINEERING

United States Naval Postgraduate School  
Monterey, California

1956

11  
B725

This work is accepted as fulfilling  
the thesis requirements for the degrees of

MASTER OF SCIENCE  
IN  
MECHANICAL ENGINEERING

from the  
United States Naval Postgraduate School



## PREFACE

"Underway on nuclear power." With this simple but historically significant message, the U.S.S. Nautilus heralded a new age in power generation. Powered by the first mobile nuclear reactor, she set the stage for dramatic developments in military and industrial fields. A powerful vessel, but unwieldy and undesirably large for a submarine, her size was largely determined by the size of the power plant components. One of the more significant of these components is the pressurizer for the reactor primary coolant system. This tank is extremely large due to the conservative design necessitated by ignorance of the thermodynamic transient behavior in its pressure range.

The objective of this thesis is to produce design data for steam pressurizing systems, by electronic analog simulation of the thermodynamic transients which occur in the pressurizer vessel.

The writers wish to thank Professor Eugene E. Drucker, and Professor Hugo M. Martinez of the U.S. Naval Postgraduate School for their assistance and enthusiastic cooperation in the prosecution of this project.





# TABLE OF CONTENTS

Item	Title	Page
Chapter I	Introduction . . . . .	1
Chapter II	Development of Theoretical Equations . . . . .	4
Chapter III	Application of Equations to the Analog Computer . . . . .	10
Chapter IV	Analog Computer Solution of Theoretical Equations . . . . .	14
Chapter V	Experimental Results and Conclusions . . . . .	19
Bibliography	. . . . .	29
Appendix I	Derivation of Empirical Relations for Pressure and Compressibility Factor . . . . .	30
Appendix II	Derivation of Machine Equations. . . . .	40
Appendix III	Hand Solution of Theoretical Equations . . . . .	44
Appendix IV	Actual Tank Transient Data . . . . .	50



# LIST OF ILLUSTRATIONS

Figure		Page
1.	Boeing Electronic Analog Computer and Sanborn Recorder . . . . .	3a
2.	Equivalent System . . . . .	4
3.	Block Diagram of Computer Circuit. . . . .	11
4.	Hand Solution Curves . . . . .	15
5.	Sanborn Recording of Test Run. . . . .	16,17
6.	K Determination for Typical Run. . . . .	20
7.	K - Surge Duration Diagram . . . . .	22
8.	Pressure Prediction Curves . . . . .	25
9.	Temperature- Entropy Chart . . . . .	26
10.	Enthalpy - Pressure. . . . .	31
11.	Internal Energy - Pressure . . . . .	33
12.	Constant - Specific Volume, for e computation. . .	35
13.	Compressibility Factor - Pressure Diagram. . . . .	37
14.	Constant - Specific Volume, for Z computation. . .	39
15.	Computer Schematic Diagram . . . . .	43



# TABLE OF SYMBOLS AND ABBREVIATIONS

a	potentiometer setting for analog computer
C	capacitance in micro-farads
c	mathematical constant
$c_p$	specific heat
E	total internal energy in B.T.U.
e	specific internal energy in B.T.U. per pound
$^{\circ}\text{F}$	temperature in degrees Fahrenheit
H	total enthalpy in B.T.U.
h	specific enthalpy in B.T.U. per pound
I.C.	initial conditions
J	energy conversion factor, equal to 778 ft lb/BTU
K	effective thermal conductance
k	mathematical constant
lb.	pound
M	megohms resistance
m	mass
P	absolute pressure
p.p.	patch panel (analog computer)
Q	total heat energy in B.T.U.
q	specific heat energy in B.T.U. per pound
R	electrical resistance
$^{\circ}\text{R}$	temperature in degrees Rankine
T	absolute temperature
t	time in seconds



$\Delta t$	duration of surge in seconds
$u$	amplitude of driving function, equal to one-half the change in spec. volume during a surge
$V$	total volume of steam in cubic feet
$v$	specific volume in cubic feet per pound
$W$	total work done on system in B.T.U.
$w$	specific work in B.T.U. per pound
$Z$	compressibility factor
$\alpha$	scaling factor for analog computer
$\omega$	natural frequency in radians per second

#### SUBSCRIPTS

$o$	initial value
$e$	pertains to internal energy
$f$	final value
$p$	pertains to pressure
$q$	" " heat energy
$s$	" " steam
$T$	" " temperature
$t$	" " time
$v$	" " specific volume
$w$	" " work
$z$	" " compressibility factor





## SUPERSCRIPTS

$\overline{P}$	a bar over any symbol represents the voltage equivalent to that quantity (analog computer)
$\dot{w}$	a dot over any symbol indicates the first derivative of the quantity with respect to time

## OPERATORS

$d$	exact differential of a quantity
$\int_p$	exact integral of a quantity (Heaviside notation)



# CHAPTER I

## INTRODUCTION

The prototype (Mark I) of the Submarine Thermal Reactor (STR) was the first full scale power reactor in the world to be completed and successfully operated. The first central station nuclear power plant in the United States will be the Pressurized Water Reactor (PWR), nearing completion at Shippingport, Pennsylvania. The many highly desirable aspects of the pressurized light water reactor cause it to be one of the most promising types, to date.

A basic requirement for these light water reactors is that a very high pressure is maintained on the primary coolant. Pressures in the neighborhood of 2000 psia and higher are presently in use. High pressures permit the use of sub-cooled water at high temperatures in the reactor without danger of boiling.

When any control program other than constant average primary loop temperature is used, a change in the volume of the primary coolant is to be expected for a corresponding change in power. A volumetric transient is consequently induced and a surge tank is required in the system. Since the primary coolant must be maintained at a high pressure the surge vessel is also used to perform this function.

The pressurizer must be strong enough to maintain steam and water in equilibrium at high pressures. It must be large enough to absorb normal and accidental surges without permitting excessive pressures in the primary loop. Although thermally insulated, it must have internal heaters, capable of maintaining the water and steam at the saturation



temperature. These heaters must have additional heating capacity capable of generating steam at sufficient rate so as to prevent excessive pressure drop in the primary coolant during negative (out) surges.

Specifically, in this thesis we will assume a primary loop working pressure of 2000 psia, normal volume surges of 4 cubic feet and accidental surges of 7 cubic feet as representative values. At steady state water and steam are maintained at saturation temperature (636 °F) in the tank, but only the pressure (2000 psia) is transmitted to the cooler primary loop via a relatively long stand-pipe. Assuming that the installed heaters adequately compensate for negative surges, this type surge is not considered a design limitation. Therefore only those surges caused by an increase in primary loop volume, or positive surges, will be considered here.

When designing or sizing a pressurizer, limits must be imposed on the various properties of the fluids in the tank. The maximum allowable pressure change must be determined from consideration of the strength of the members involved. The expected change in average density and therefore volume of the primary coolant must be computed. The duration of the surge is determined from changes in power, either accidental or deliberate. The one remaining variable, the size of the tank must now be determined on the basis of the aforementioned parameters.

The pressure change caused by a positive surge may be minimized by introducing a portion of the surge water into the top of the tank as a finely divided spray. The most conservative basis for pressurizer design is to assume that no spray is employed, the steam is dry saturated,



and undergoes isentropic compression. Should the steam not be dry, the resulting final pressure would be lower than in the case of dry steam. The optimum and therefore minimum size required can only be positively determined after a complete understanding of the thermodynamic and heat transfer mechanisms involved.

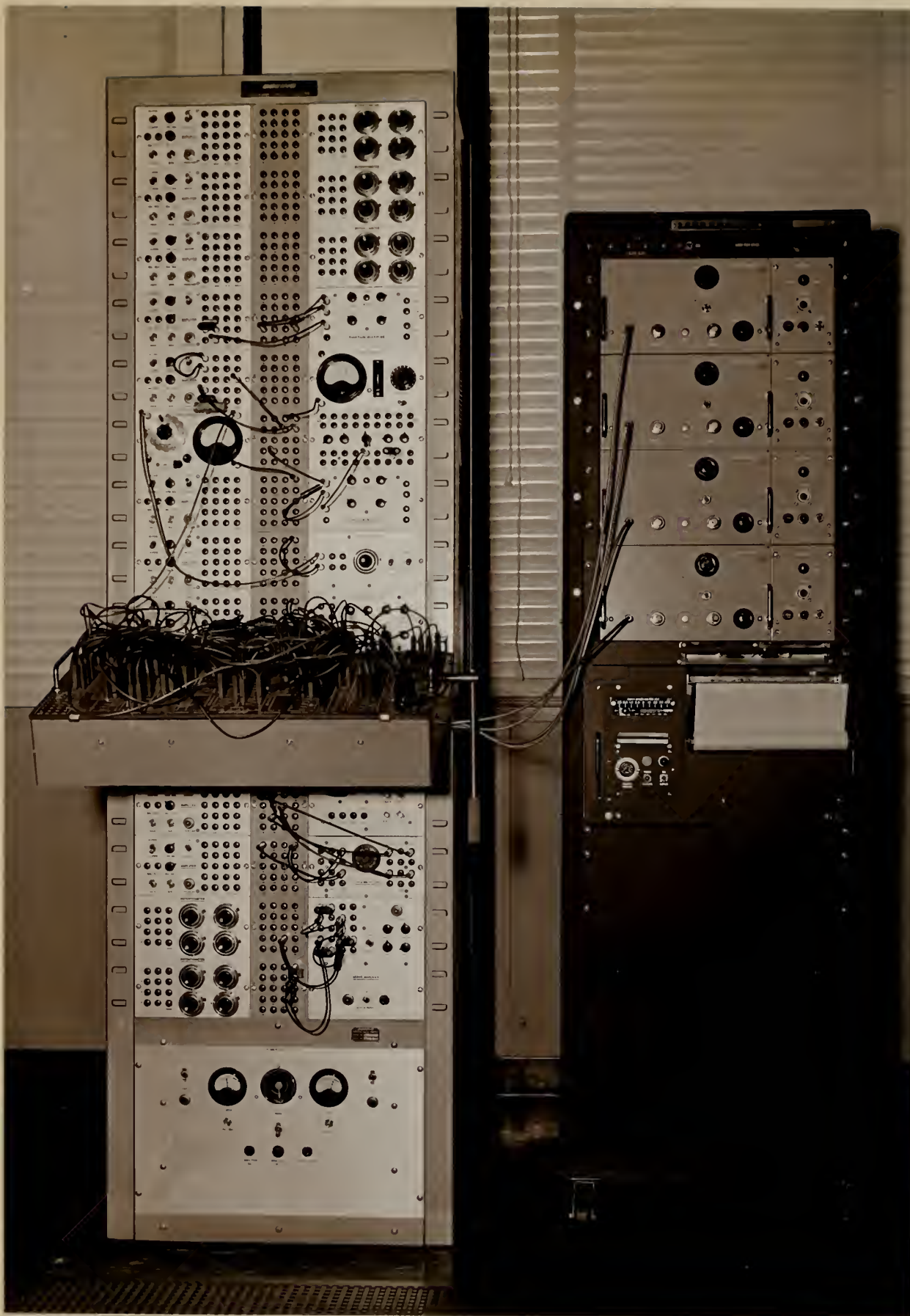
In this project, it is felt that valuable information is available, both in the fields of design limitation and in determining the characteristics of high pressure saturated steam. A Boeing Electronic Analog Computer with associated 4-channel Sanborn Recorder (see Fig. 1) is utilized to simulate the pressurizer, with the above objectives in view.

An important assumption which is made at the outset is that the driving function, specific volume (which is directly related to tank level) follows a cosine curve. Analysis of actual tank transients indicates that this approximation is a good one for a large portion of them. This type of function can be easily produced on the analog computer, while production of more exact functions is difficult.

In the analysis of results, every attempt is made to utilize the principle of geometric similarity, to more nearly generalize these results.







BOEING ELECTRONIC ANALOG COMPUTER AND SANBORN RECORDER

Figure 1

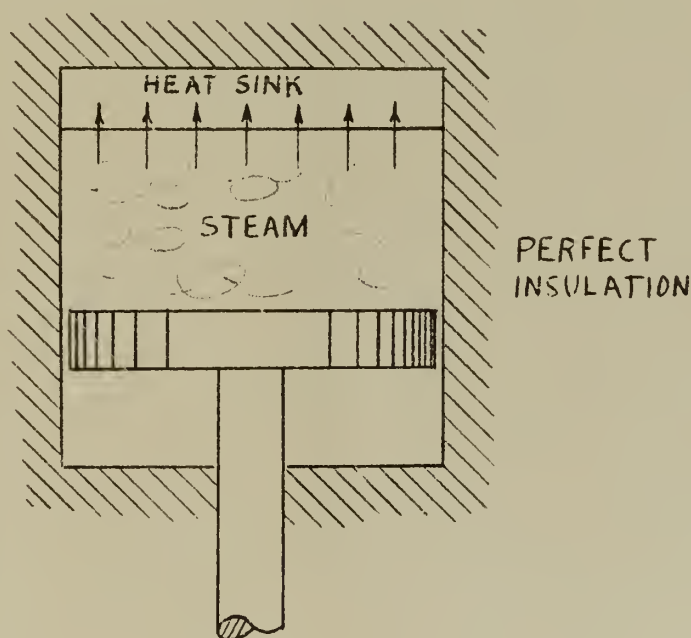


## CHAPTER 11

### DEVELOPMENT OF THEORETICAL EQUATIONS

The initial step in the analog simulation of this problem consists of a description of the system in terms of theoretical equations. Whenever possible known thermodynamic relationships are used, and when this is not possible empirical relationships are developed. No reference can be found in the literature treating the following development of descriptive equations, and it is believed that this approach may be a new one.

As an initial simplifying assumption, an equivalent system is devised which lends itself more readily to analysis than does the actual tank.



Equivalent System

Figure 2



The actual tank is well insulated, therefore the concept of perfect insulation for the equivalent arrangement does not introduce significant error. The thermodynamic system is defined as the mass of steam in the tank. In the actual tank there is installed internally a spray and degasifier assembly. In this analysis of positive surges, without spray, its only effect is to function as a heat sink. The heat sink in the equivalent arrangement represents the tank walls, spray and degasifier assembly, the mass of water in the tank, and all other apparatus within the tank insulation. The piston represents the water surface, which in the actual tank performs work upon the steam during an in-surge. Thermodynamic equilibrium is assumed at all times.

Equation #1 is the well-known work equation:

$$w = -\int P \, dv$$

where  $w$  = work (BTU/lb), positive when work is done on the system

$P$  = system pressure (psia)

$v$  = specific volume of steam (cubic feet/lb)

Considering units,

$$w = -\frac{144}{J} \int P \, dv = -.1853 \int P \, dv$$

In Heaviside operator form,

$$w = -\frac{1}{p} \left[ .1853 P \left( \frac{dv}{dt} \right) dt \right] = -.1853 \int P \left( \frac{dv}{dt} \right) dt$$

Equation #2 is the First Law of Thermodynamics:

$$\Delta e = q + w$$

or  $e = q + w + e_0$

where  $e$  = specific internal energy (BTU/lb)

$q$  = heat flow (BTU/lb), positive when into the system





Equation #3 is the equation of state for a non-ideal gas:

$$Pv = c_1 Z T$$

where  $Z$  is defined as  $\frac{Pv}{c_1 T}$  (dimensionless compressibility factor)

$T$  = absolute temperature ( $^{\circ}R$ )

$$c_1 = \frac{1545}{18.01 \times 144} = .5957 \frac{\text{lb}_g \text{ ft}^3}{\text{in}^2 \text{ lb}_m ^{\circ}R} \quad (\text{gas constant})$$

Equation #4 relates  $P$  to  $e$  and  $v$  empirically from steam table values (see Appendix I):

$$P = 8.51 e + 52,590 v^2 - 30,700 v - 3161$$

Equation #5 relates  $Z$  to  $P$  and  $v$  empirically, in the saturated and superheated region, from steam table values (see Appendix I):

$$Z = 1.715 \times 10^{-4} P - 9.47 v^2 + 6.048 v - .5693$$

Note: Equation #5 is not required mathematically, but is desirable for computer circuit simplicity.

Equation #6 relates heat flow to temperature differences and is developed as follows:

First, consider the sink as a system,

$$dQ_{\text{sink}} = m_{\text{sink}} c_{\text{sink}} dT_{\text{sink}}$$

where  $Q_{\text{sink}}$  = quantity of heat energy (BTU)

$m_{\text{sink}}$  = mass of sink (lb)

$T_{\text{sink}}$  = temperature of sink ( $^{\circ}R$ )

$c_{\text{sink}}$  = sink heat capacity (BTU/lb $^{\circ}R$ )

Rearranging,

$$dT_{\text{sink}} = \frac{1}{m_{\text{sink}} c_{\text{sink}}} dQ_{\text{sink}}$$





Integrating,

$$T_{\text{sink}} = \frac{1}{m_{\text{sink}} c_{\text{sink}}} Q_{\text{sink}} + (T_o)_{\text{sink}}$$

but  $Q_{\text{steam}} = -Q_{\text{sink}} = Q$

and  $(T_o)_{\text{steam}} = (T_o)_{\text{sink}} = T_o$

Then,

$$T_{\text{sink}} = \frac{-1}{m_{\text{sink}} c_{\text{sink}}} Q + T_o$$

Now, considering the original system (the steam):

$$\frac{dQ}{dt} = -K (T - T_{\text{sink}})$$

K represents the effective thermal conductance of the system boundary, and will be considered a constant in the equivalent system for any given surge. The units of K are (BTU/sec<sup>°R</sup>). K is ordinarily the product hA, when each is determinable.

Substituting for  $T_{\text{sink}}$ ,

$$\frac{dQ}{dt} = -K \left( T + \frac{Q}{m_{\text{sink}} c_{\text{sink}}} - T_o \right)$$

Since  $Q = m_s q$ , where  $m_s$  = mass of steam (lb)

$$\frac{dq}{dt} = -\frac{K}{m_s} (T - T_o) - \frac{K}{m_{\text{sink}} c_{\text{sink}}} q$$

The problem which is now encountered is that of evaluating the equation constants. Since accurate design data are not available, these constants must necessarily be evaluated in an arbitrary and approximate manner.

For the subject tank,  $m_{\text{sink}}$  can be taken as 3000 lb. This is approximated as follows:



mass of metal  $\approx$  2000 lb.

mass of water  $\approx$  1000 lb.

Total 3000 lb.

The heat capacity of water at the pressure and temperature range involved is approximately 2.0 BTU/lb<sup>o</sup>R . The heat capacity of stainless steel (tank wall material) is approximately .13 BTU/lb<sup>o</sup>R . A weighted average heat capacity of the sink is computed as follows,

$$c_{\text{sink}} = \frac{2 \times 1000 + .13 \times 2000}{3000} = .75 \text{ BTU/lb}^{\circ}\text{R}$$

The mass of steam in the system will depend on the initial tank level, and saturation conditions, but rarely varies greatly from an average value of 175 lb. Properly, the mass of steam should be computed and Equation #6 modified for every run simulated, but for simplicity this average value is used for all surges. In all simulated surges,  $m_{\text{sink}}$ ,  $c_{\text{sink}}$ , and  $m_s$  are taken as constants, while the quantity K is adjusted to cause computed transient properties to coincide with experimental data.

Equation #6 with constants evaluated becomes,

$$\frac{dq}{dt} = - 5.72 \times 10^{-3} K (T - T_o) - .445 \times 10^{-3} K q$$

In Heaviside operator notation, the equation takes the form,

$$q = - \frac{1}{p} \left[ 5.72 \times 10^{-3} K (T - T_o) + .445 \times 10^{-3} K q \right]$$

During all runs the assumption is made that the steam mass remains constant throughout the surge. Since the energy introduced as work during a surge is on the order of 3000 BTU, the maximum mass change would be in the neighborhood of 6 lb., if all of the energy were involved



in a phase change. Therefore, the percentage mass change can never be a significant value, especially since heat flows abundantly to the sink. Any phase change will significantly affect K however, because of the heat transfer mechanism involved (heat of vaporization).

The six theoretical equations as developed and in their most useful forms appear as follows:

$$\#1 \quad w = -\frac{1}{p} \left[ c_{12} P \left( \frac{dv}{dt} \right) dt \right]$$

$$\#2 \quad e = q + w + e_0$$

$$\#3 \quad T = \frac{P v}{c_1 Z}$$

$$\#4 \quad P = c_2 e - c_3 v + c_4 v^2 - c_5$$

$$\#5 \quad Z = c_6 P + c_7 v - c_8 v^2 - c_9$$

$$\#6 \quad q = -\frac{1}{p} \left[ c_{10} K (T - T_0) + c_{11} K q \right]$$

where,

$$c_1 = .5957$$

$$c_7 = 6.048$$

$$c_2 = 8.51$$

$$c_8 = 9.47$$

$$c_3 = 3.07 \times 10^4$$

$$c_9 = .5693$$

$$c_4 = 5.259 \times 10^4$$

$$c_{10} = 5.72 \times 10^{-3}$$

$$c_5 = 3161$$

$$c_{11} = .445 \times 10^{-3}$$

$$c_6 = 1.715 \times 10^{-4}$$

$$c_{12} = .1853$$



## CHAPTER III

### APPLICATION OF EQUATIONS TO THE ANALOG COMPUTER

After the derivation of the six theoretical equations, a computer circuit must be designed to accomplish their simultaneous solution. In the circuit design many things must be considered; such as, scaling factors, follow-up time of multiplier components, amplifier drift, voltage magnitudes, etc. A certain amount of latitude is allowed in circuit component selection, but definite limits are present due to stability considerations.

The six basic equations in computer notation appear as below:

$$\#1 \quad \bar{w} = -\frac{1}{p} \left[ 1.111 \left( .1P \frac{d\bar{v}}{dt} \right) \right]$$

$$\#2 \quad \bar{e} = .0333 \bar{q} + .0333 \bar{w} + \bar{e}_0$$

$$\#3 \quad \bar{T} = 3.3574 \left( \frac{\bar{P} \bar{v}}{L} \right)$$

$$\#4 \quad \bar{P} = 4.255 \bar{e} - 5.1167 \bar{v} + 4.3825 (\overline{.02 v^2}) - 52.6833$$

$$\#5 \quad \bar{L} = .5145 \bar{e} + 3.024 \bar{v} - 2.3675 (\overline{.02 v^2}) - 28.465$$

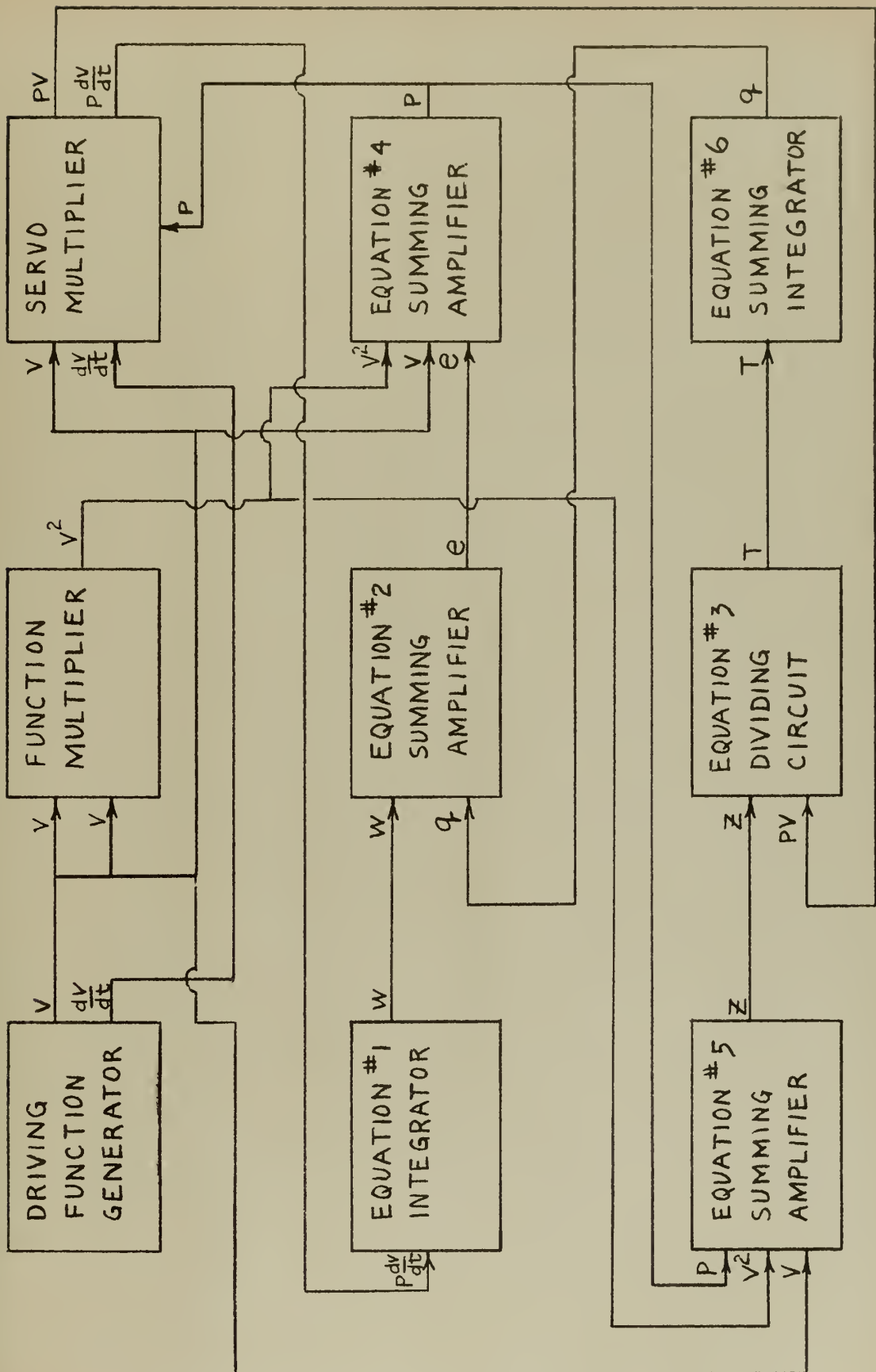
$$\#6 \quad \bar{q} = -\frac{1}{p} \left[ .1716 K \bar{T} - .1716 K \bar{T}_0 + .000445 K \bar{q} \right]$$

The bar over a quantity represents the quantity as a voltage. The detailed conversion of the theoretical equations to the above "machine" equations comprises Appendix II.

Fig. 3 shows the resulting machine circuit in block diagram form. For the detailed circuit, see Appendix II. Briefly, the circuit is designed to function as follows:







BLOCK DIAGRAM OF COMPUTER CIRCUIT  
FIGURE 3



In the driving function circuit a cosine function is added electrically to a constant voltage, the resultant voltage transient very closely approximates the specific volume throughout a surge. The amplitude of the cosine function represents one-half the change in  $v$ , while the period of the function is twice the time of the surge ( $\Delta t$ ). Within this same circuit the time derivative of specific volume,  $\frac{dv}{dt}$  is also generated.

A function multiplier is used to obtain the quantity  $\overline{v^2}$ , while a servo-multiplier produces the products  $\overline{P \frac{dv}{dt}}$  and  $\overline{P v}$ . An integrating circuit integrates  $\overline{P \frac{dv}{dt}}$  as a function of time to produce specific work,  $\overline{w}$ . Another integrating circuit produces the time integrated specific heat flow,  $\overline{q}$ , using temperature inputs.

A summing amplifier sums  $\overline{e}_0$ ,  $\overline{w}$ , and  $\overline{q}$  to produce  $\overline{e}$ . Another sums  $\overline{e}$ ,  $\overline{v}$ , and  $\overline{v^2}$  to produce  $\overline{P}$ . A third sums  $\overline{P}$ ,  $\overline{v}$ , and  $\overline{v^2}$  to produce  $\overline{Z}$ . A dividing circuit performs the division  $\frac{\overline{P v}}{\overline{Z}}$  to produce  $\overline{T}$ .

The circuit required to solve the set of equations consists of eleven amplifiers, four sign-changing amplifiers, two function multipliers, one duo-channel servo-multiplier, and twenty-one 50,000 ohm potentiometers. The net result is a rather complex circuit, but one which does not seem to be subject to further simplification without sacrificing necessary accuracy. Since instability in this type of computer is a direct function of the number of components used, circuit simplicity has been a constant objective.

This phase, the designing and setting up of the circuit, requires a great deal of computer experience and proficiency. For the uninitiated, many trial and error situations are encountered, and with a circuit of



this complexity the process can be very time consuming.

The following chapter will deal with the problem of producing quantitative results, assuming the circuit has been designed, balanced and tested.



## CHAPTER IV

### ANALOG COMPUTER SOLUTION OF THEORETICAL EQUATIONS

After the analog computer circuit is designed, assembled, and rough qualitative results obtained, the next phase consists of producing accurate quantitative solutions. The first step in accomplishing this, consists of static adjustment. With various initial values of  $e_0$ , and  $v$  set, the  $e$ ,  $P$ ,  $Z$  and  $T$  computing circuits are adjusted to give steam table values for these quantities over the entire anticipated range. This step of the computer set-up is very exacting and time consuming but is a necessary step prior to adjusting for dynamic accuracy.

Prior to the dynamic adjustment, a hand solution of the system of theoretical equations is obtained for use as an adjustment reference. A set of initial conditions, and a driving function are arbitrarily selected, and using the Heun Method<sup>1</sup> of numerical integration, a point-by-point solution of the equations is calculated (see Appendix III). The various thermodynamic quantities as calculated are plotted, the resulting curves serving as the final reference for dynamic adjustment (see Fig. 4).

Next, the computer is made to duplicate the hand solution. This is done by adjusting the  $w$  and  $q$  integrating circuits until the  $w$  and  $q$  curves, as viewed on a properly calibrated Sanborn Recorder, are of the proper shape and magnitude (see Fig. 5). These adjustments in general are minor.

The value of careful static adjustment is now apparent since no further adjustment of the  $e$ ,  $P$ ,  $Z$  and  $T$  circuits is found necessary.

<sup>1</sup> Special case of Runge-Kutta Method; see Kopal, Numerical Analysis, pp. 202-205, Wiley (1955).





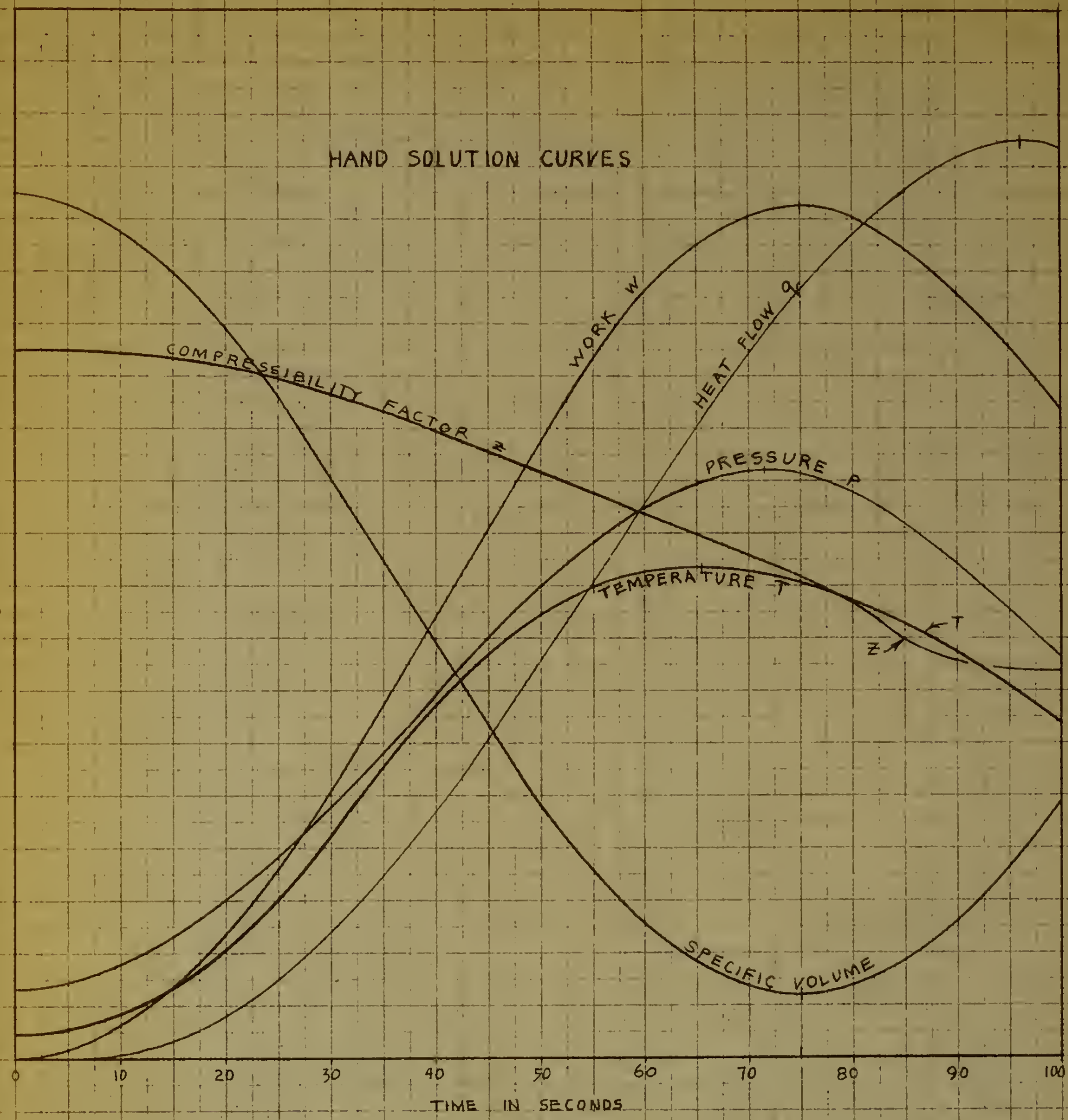
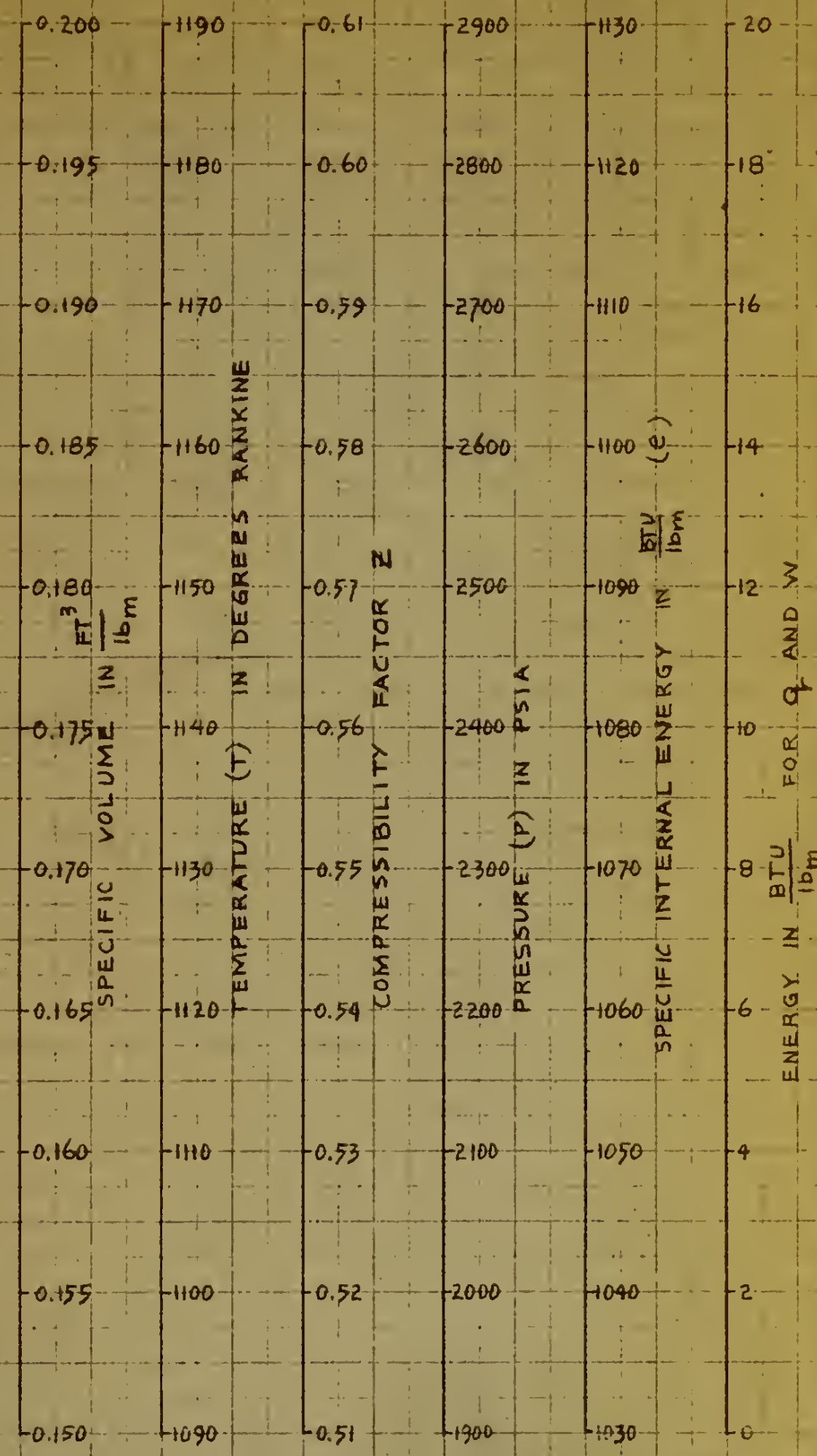
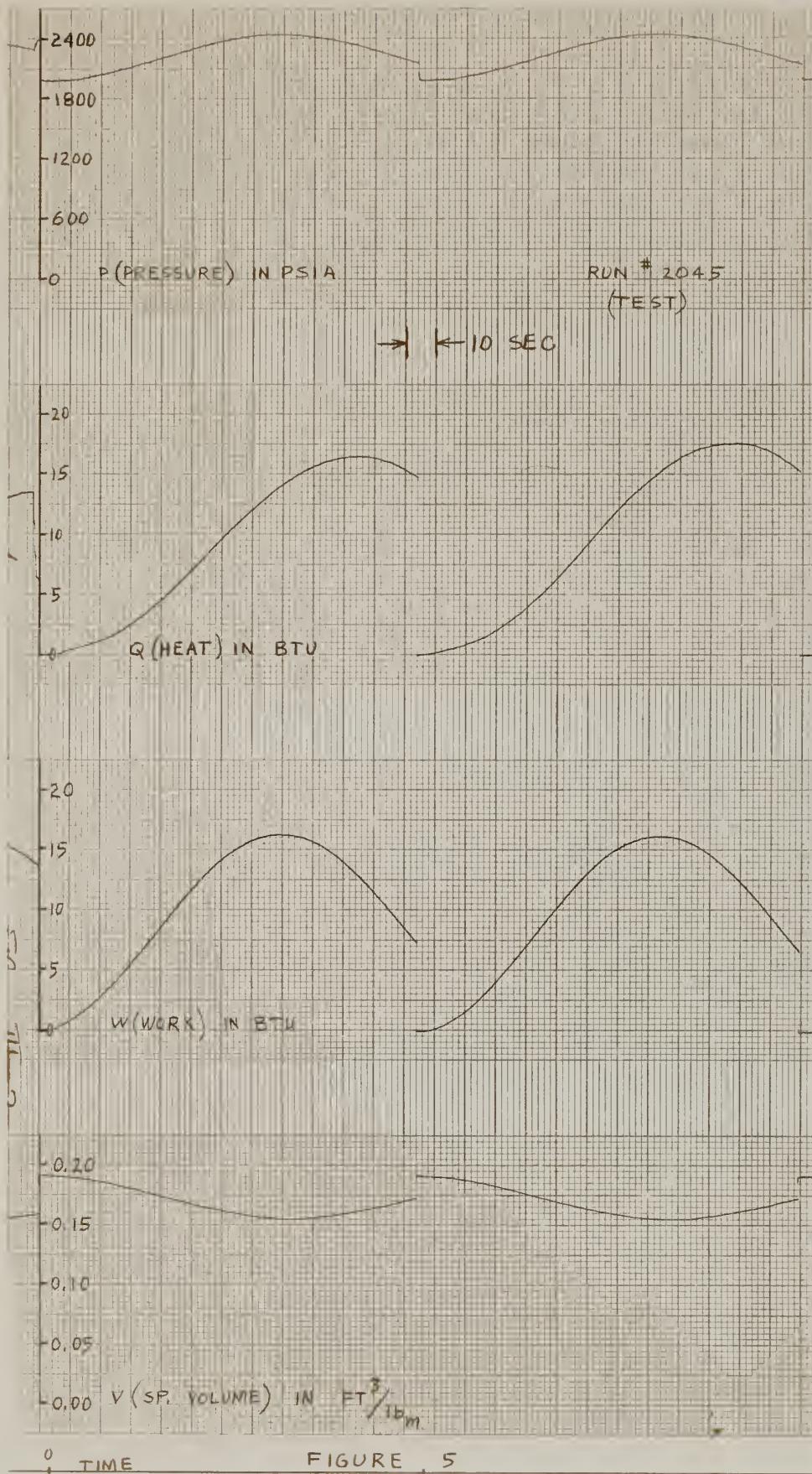


FIGURE 4











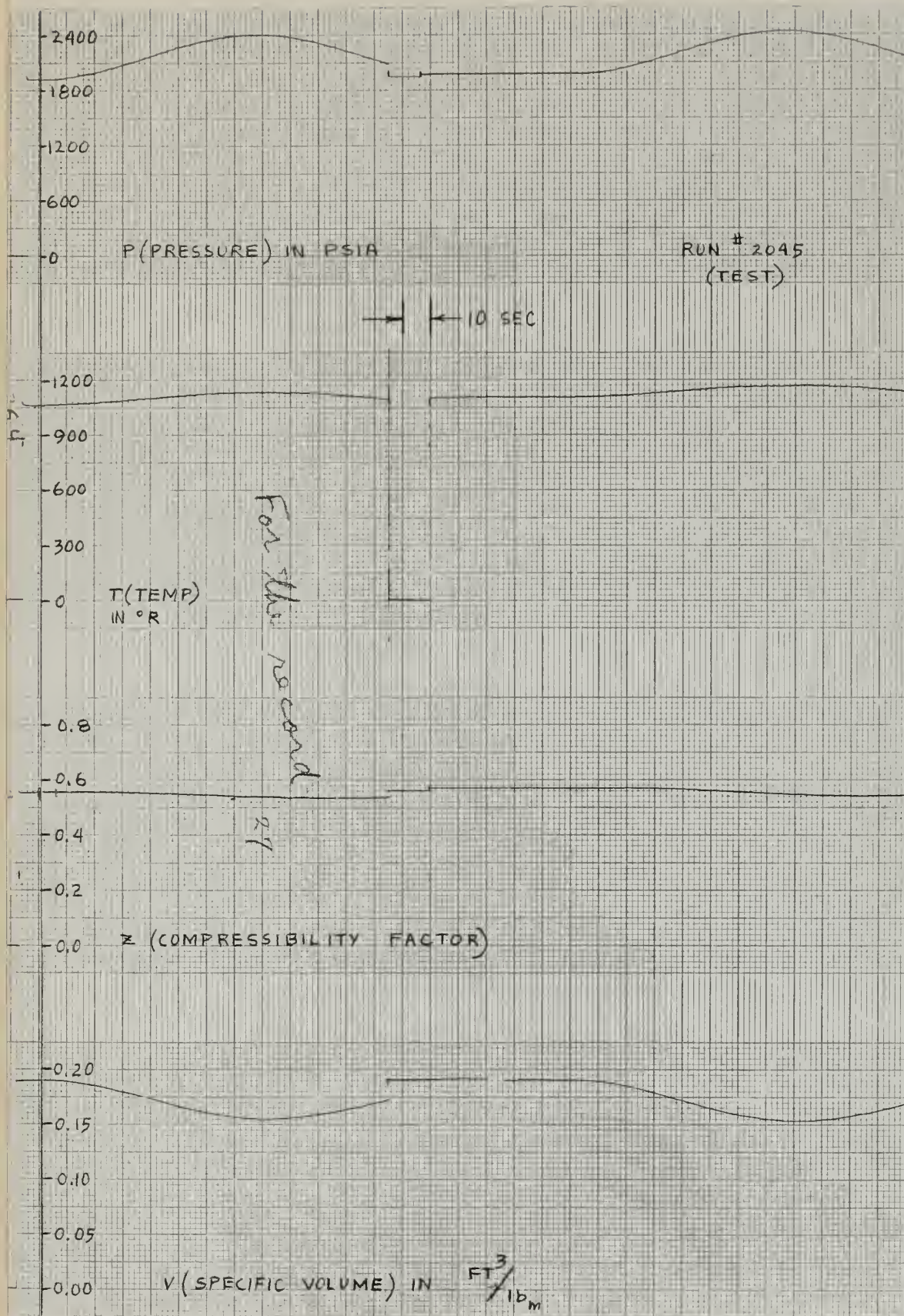


FIGURE 5 (CONT.)



The curves of these quantities are now found to match the corresponding hand solution curves very well (see Figs. 4 and 5).

Once the hand solution is duplicated, a reference for measuring K is now available. In the hand solution, the arbitrarily selected value of K is .9254. The corresponding setting of potentiometer  $a_{14}$  is now readily observed (usually in the neighborhood of .100, varying slightly from day to day). Since K and the  $a_{14}$  setting are proportional, K can be determined at any time by the simple relation,

$$K = K_0 \times \frac{(a_{14})}{(a_{14})_0}$$

It is now possible to vary K over a large range of values by merely adjusting a single potentiometer, thus varying the integrated  $q_1$  curve, and all other curves of thermodynamic properties. By simulating the driving function for a given surge, K can be varied until the proper pressure curve is obtained (i.e. a pressure curve which matches the pressure curve resulting from an actual tank transient). The next chapter discusses the investigation of actual surges by simulator, to determine values of K for these surges. Correlation of K with surge types is also discussed.





## CHAPTER V

### EXPERIMENTAL RESULTS AND CONCLUSIONS

Appendix IV is a compilation of data obtained from the actual surge tank. Eighteen positive surges are represented, spray being utilized in only one. It is evident that possession of many more runs would be desirable, but the present number must suffice since more could not be obtained. Fortunately these eighteen surges represent a fair cross-section of positive surges encountered.

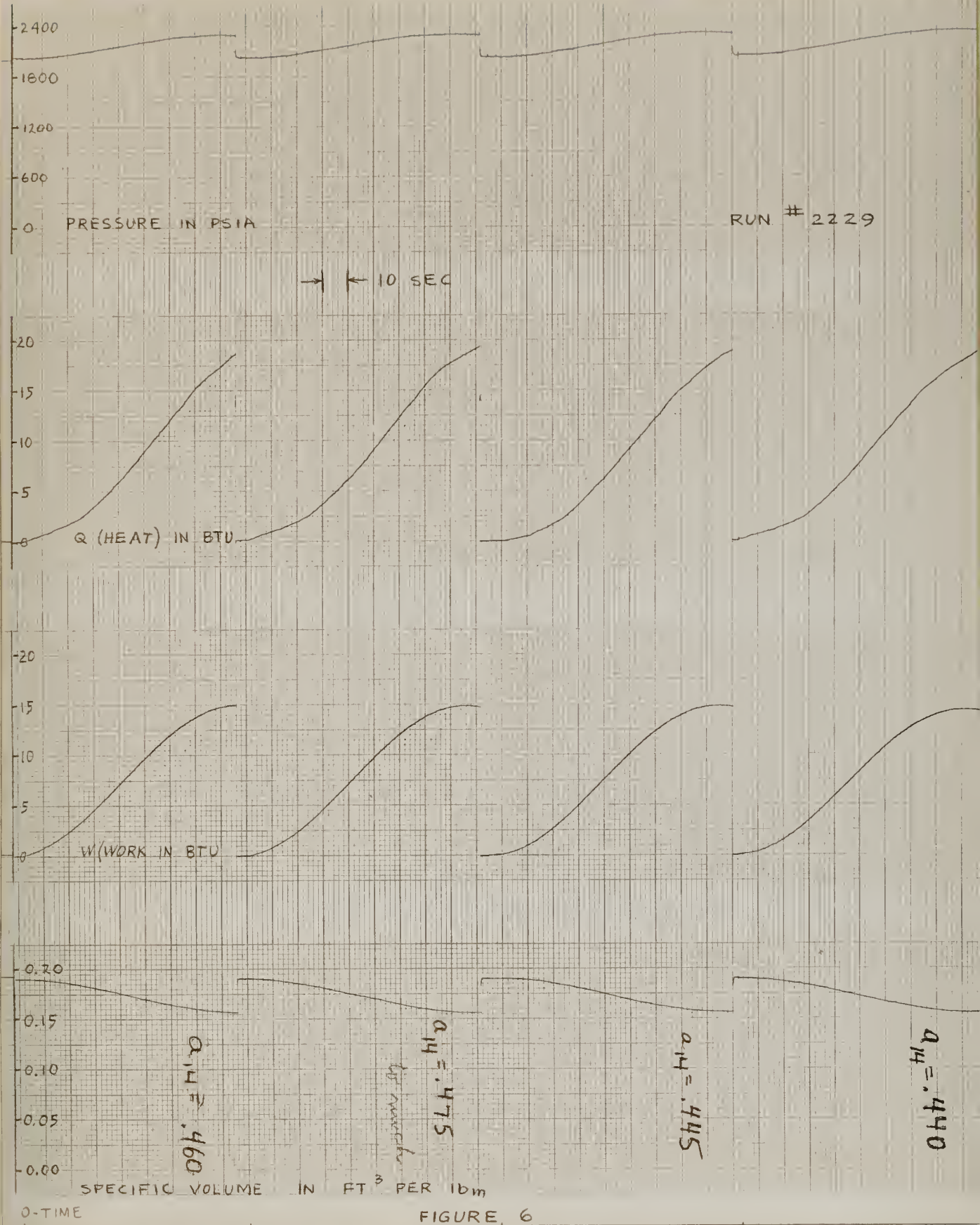
The procedure for simulating a given surge is outlined in Chapter IV and briefly is as follows:

A proper driving function (specific volume) is set up on the computer, providing for the generation of a cosine curve of proper amplitude and period. Initial values of  $v$ ,  $e$ ,  $T$ , and a trial value of  $K$  are set, and a surge is generated.  $K$  is adjusted for several trials until the generated property curves match the corresponding actual tank curves (see Fig. 6 for Sanborn recording of this procedure).

Each of the eighteen surges is simulated in this manner, and the proper value of  $K$  determined (see Table 1). Many attempts at correlating  $K$  with various quantities ( $\Delta v$ ,  $\frac{\Delta v}{v_0}$ ,  $\frac{\Delta v}{\Delta t}$ , etc.) were fruitless, but a fair correlation with surge duration ( $\Delta t$ ) is possible (see Fig. 7). It is likely, in fact, that  $K$  is a function of several or all of the variables considered, but the effect of each seems small in comparison to the effect of  $\Delta t$ . By simple curve fitting, a correlating equation is derived,

$$K = 3.75 + \frac{25}{t - 17}$$





K DETERMINATION FOR TYPICAL RUN



Nothing is claimed for this equation except that it describes a  $K$  which aids in predicting pressure rises on the safe side (i.e. in most cases the predicted pressure rise will be somewhat larger than the actual pressure rise). Column 4 of Table 1 lists the  $K$  for each surge as predicted by formula.

In general, it can be observed that  $K$  does not vary greatly for any surge of over 30 seconds duration, and that it becomes nearly constant for surges longer than 90 seconds. It is also true that pressure rise is not sensitive to moderate changes in  $K$ . The last column of Table 1 lists errors encountered when a constant value of 3.75, the limiting value of  $K$ , is used in the computer.

The mechanism of heat transfer for the actual tank can only be surmised. However, it is logical to expect greater turbulence for shorter, faster surges, resulting in somewhat larger values for  $K$ . This could be due to a larger heat transfer surface between the steam and water in the tank. The effectiveness of spray in increasing  $K$  is readily observed in run 1506, Table 1. Whereas a  $K$  of approximately 5.0 could have been expected without spray, the actual  $K$  observed is 13.8 .

From the general characteristics of the  $K$  vs. Surge Duration curve (Fig. 7), it appears that  $K$  approaches a limiting value of about 3.75 for surges of long duration. For geometrically similar tanks utilizing the same pressure range, the same limiting value of  $K$  could reasonably be expected.

Realizing that a correlation exists between  $K$  and the driving function, it is now possible to predict pressure rises for all conceivable driving functions. This is done in the following manner:





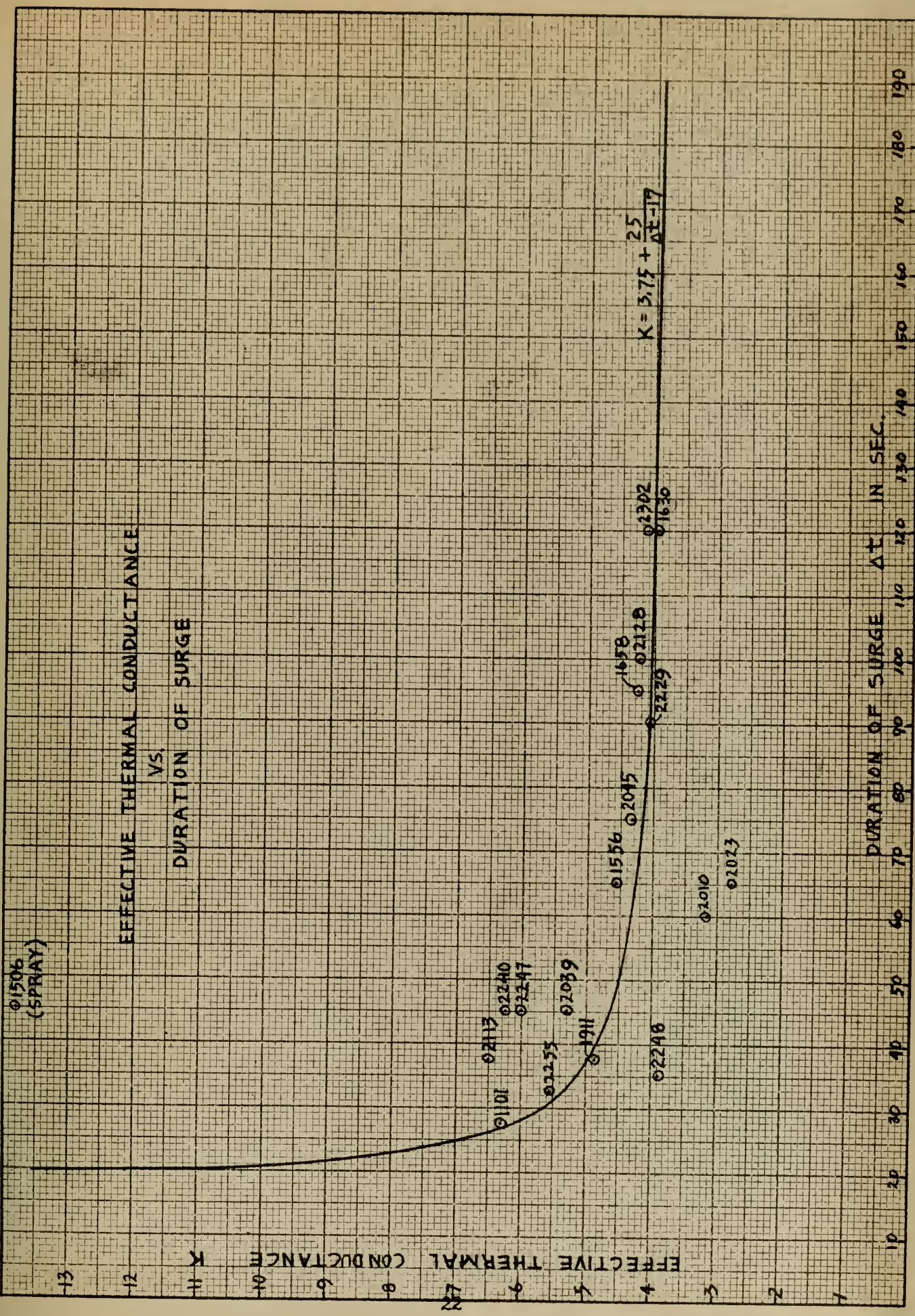


FIGURE 7





TABLE 1

RUN NO.	SLUG TIME (sec.)	k (exp.)	k (form.)	Error*
2045	75	4.31	4.17	7
2302	120	4.12	4.00	- 4
1630	120	3.96	4.00	-12
2128	100	4.26	4.05	- 5
1658	95	4.26	4.06	18
2229	90	4.07	4.07	-22
2023	65	2.78	4.27	-34
1556	65	4.54	4.27	12
2010	60	3.15	4.32	-21
1101	27.5	6.30	6.15	30
2240	45	6.25	4.65	12
2255	32.5	5.55	5.35	18
2248	35	3.90	5.15	7
1911	37.5	4.86	5.00	66
2113	37.5	6.50	5.00	60
2039	45	5.30	4.65	66
2247	45	6.02	4.65	90
1506 (spray)	45	13.8	4.65	200

\* Error in predicting pressure rise (in psia) when using a constant value of K, (the limiting value of 3.75), rather than the experimental or formula values.



A driving function is established, the proper value of  $K$  is set, and the resulting pressure rise recorded. In an attempt to use the principle of geometric similarity, dimensionless parameters are used when possible. Accordingly, a family of curves is obtained relating  $\frac{\Delta v}{v_o}$ ,  $\frac{\Delta P}{P_o}$ , and  $\Delta t$  (see Fig. 8).

Since the actual tank surges vary from 27.5 seconds to 120 seconds, the predictions are only valid within this range. However it appears that safe extrapolations may be made. An attempt to justify limiting values of the prediction curves is based on the following reasoning:

Initially the system consists of dry saturated steam. As a surge progresses work is done on the system, and heat will flow out provided a temperature difference exists. Examination of Fig. 9 shows that the isentropic compression process prescribes the practical upper limit of over-pressure. It is believed that a process following the saturation line prescribes the lower limit of over-pressure for this tank. Since the surge introduces colder water into the tank, a potential sink exists which could conceivably cause the process to enter the wet steam region. However, a careful study of actual surges indicates that the steam remains superheated throughout an in-surge. Very long surges appear to parallel closely the saturated line with slight superheat. In addition, all surges appear to be initially isentropic in nature.

Based on the above reasoning and actual test results, it is believed that the prediction curves approach finite values as  $\Delta t$  approaches infinity. The limiting value of  $\frac{\Delta P}{P_o}$  (for any given  $\frac{\Delta v}{v_o}$ ) is that which would be obtained in a process following the saturation line.





# PRESSURE PREDICTION CURVES

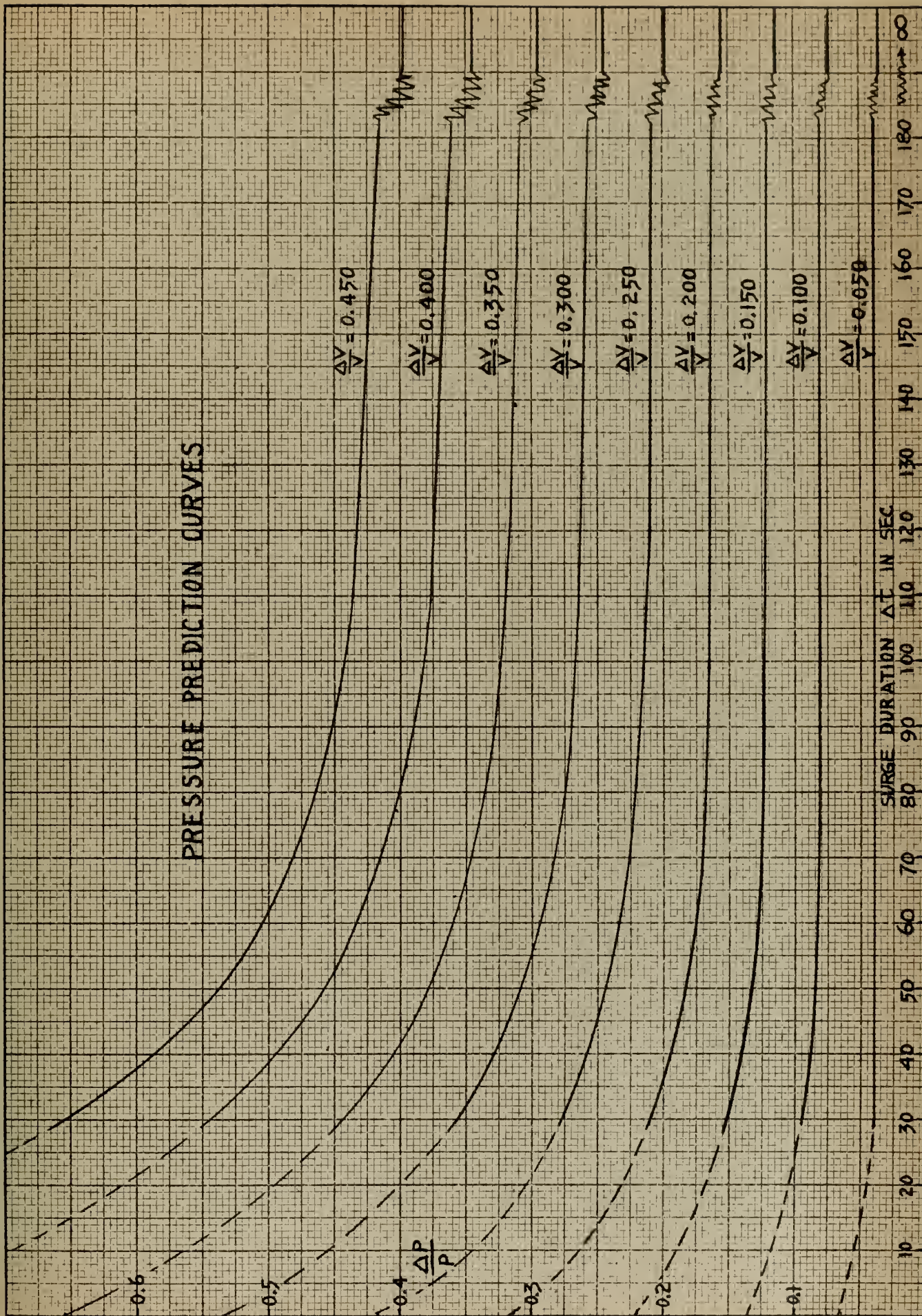
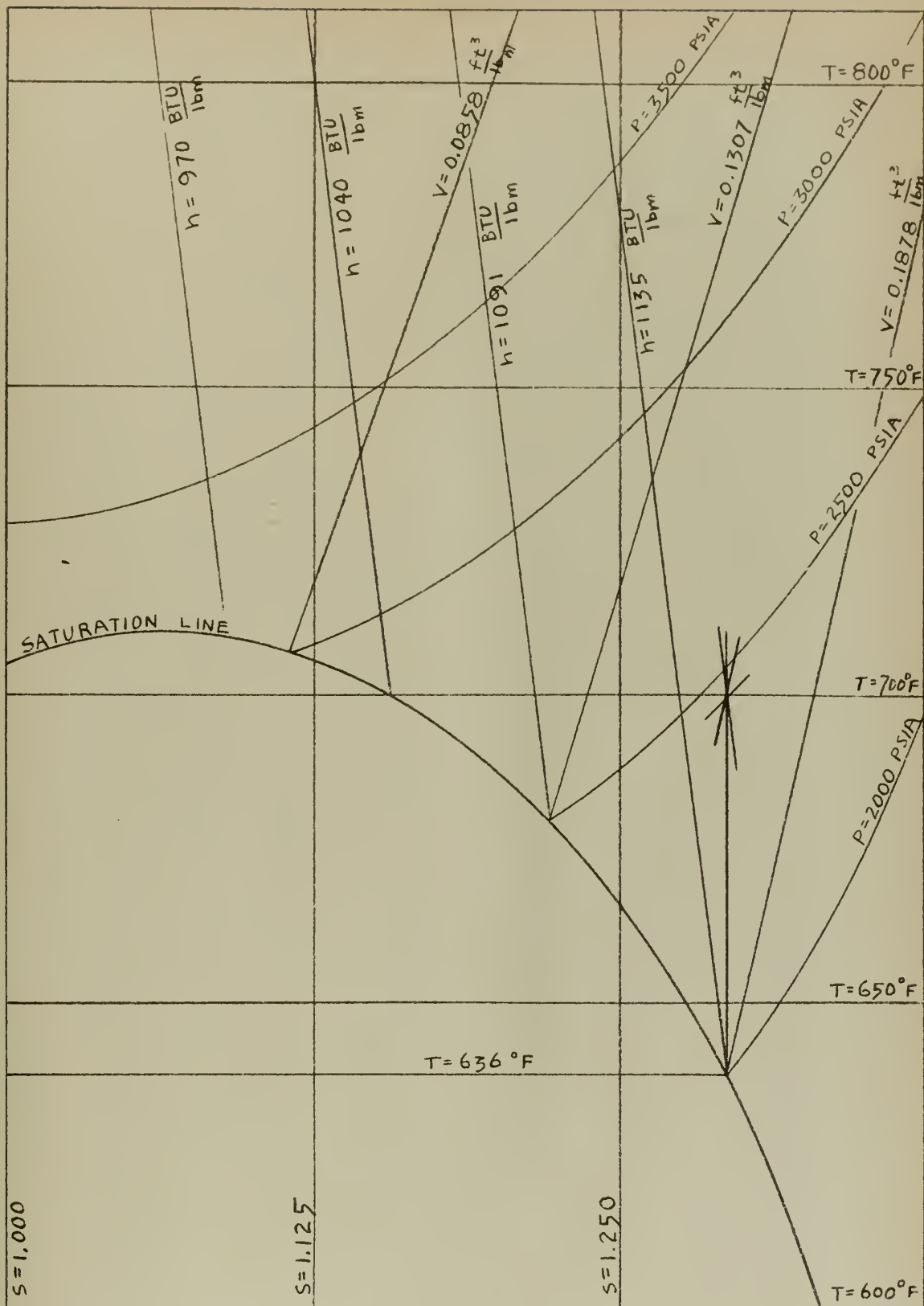


FIGURE 8







TEMPERATURE - ENTROPY CHART (APPROXIMATE)

FIGURE 9





For very short surges, the limiting condition appears to be one of isentropic compression, thus establishing a maximum value of  $\frac{\Delta p}{p_0}$  for any given  $\frac{\Delta v}{v_0}$ . On the actual installation, surges of less than 10 seconds duration are unlikely due to primary loop circulation time considerations. Thus the extrapolated curves for values of  $\Delta t$  from 10 seconds to 30 seconds would seem reasonable. Using the prediction curves (Fig. 8), Table 2 shows a comparison of predicted and actual pressure rises.

It is believed that basic objectives of this project have been realized; however many avenues for further study appear to be open. Although a procedure for rational analysis has been indicated, it appears that a study of the effect of spray, and of negative surges, by these methods would be of value.

In the field of heat transfer, a great deal remains to be done. The combining of all heat transfer mechanisms into a single coefficient is perhaps an over-simplification, although effective in this analysis. It is known that several thermal paths exist, and a more complete analysis could perhaps isolate the effects of each. Heat can flow from steam to metal, from steam to water (directly or by condensation), and from metal to water. A comprehensive simulator study could provide knowledge in this relatively unexplored field.



TABLE 2

RUN NO.	PREDICTED P (psia)	ACTUAL P (psia)	PREDICTION ERROR (psia)
2302	179	174	5
2045	317	313	4
2128	310	300	10
1556	236	229	7
2229	298	303	- 5
1506	302	289	13
2023	214	242	-28
2010	212	232	-20
2248	257	261	- 4
2240	130	110	20
2247	380	314	66
2113	150	187	-37
1101	139	112	27
2255	179	152	27
1911	420	417	3
1658	335	310	25
1630	329	324	5
2039	362	341	21



## BIBLIOGRAPHY

1. Kiefer, P.J.,  
Winney, G.F., and  
Stuart, M.C.                      PRINCIPLES OF ENGINEERING THERMODYNAMICS,  
2nd Edition, Wiley, 1954
2. Keenan, J.H., and  
Keyes, F.G.                      THERMODYNAMIC PROPERTIES OF STEAM,  
Wiley, 1936
3. Jakob, M., and  
Hawkins, G.A.                      ELEMENTS OF HEAT TRANSFER AND INSULATION,  
2nd Edition, Wiley, 1952
4. McAdams, W.H.                      HEAT TRANSMISSION, 3rd Edition,  
McGraw-Hill, 1954
5. Wheeler, R.C.H.                      BASIC THEORY OF THE ELECTRONIC ANALOG  
COMPUTER, Donner Scientific Co., 1955



## APPENDIX 1

### DERIVATION OF EMPIRICAL RELATIONS FOR PRESSURE AND COMPRESSIBILITY FACTOR

Since  $e$  can be computed from the First Law,  $e = q + w + e_0$  and  $v$  is available as a driving function, it is convenient to express  $P$  as a function of  $e$  and  $v$ . This can be done by constructing an empirical relationship from steam table values, which will be accurate within certain limits. The pressure range which is considered significant for this problem is 1700 - 2700 psia, and no accuracy is claimed beyond these limits.

Since  $e$  cannot be taken directly from the steam tables in the superheat region, a plot of enthalpy vs. pressure is made initially, showing lines of constant temperature and constant superheat (see Fig. 10).

Next, at various temperatures, various values of  $h$ ,  $P$ , and  $v$  are listed. For each of these values  $e$  is computed from the relation  $e = h - \frac{144}{J} P v$  (see Table 3). From this table, a new chart is constructed relating  $e$ ,  $P$ ,  $v$  and  $T$  (see Fig. 11). Using this chart as a basis, initially an expression for  $e = f(P, v)$  is obtained in the following manner:

The average slope of constant  $v$  lines is .1176. For any one line,  $e = .1176 P + c_{14}$ . The constant  $c_{14}$  is determined as a function of  $v$  (see Table 4 and Fig. 12),  $c_{14} = 1562 v + 538$ . The resulting expression for internal energy,  $e = .1176 P + 1562 v + 538$ , when tested at the extreme limits is found to give considerable error. Although undesirable from the standpoint of computer circuitry, an





ENTHALPY VS. PRESSURE  
WITH LINES OF CONSTANT  
SUPERHEAT AND  
TEMPERATURE

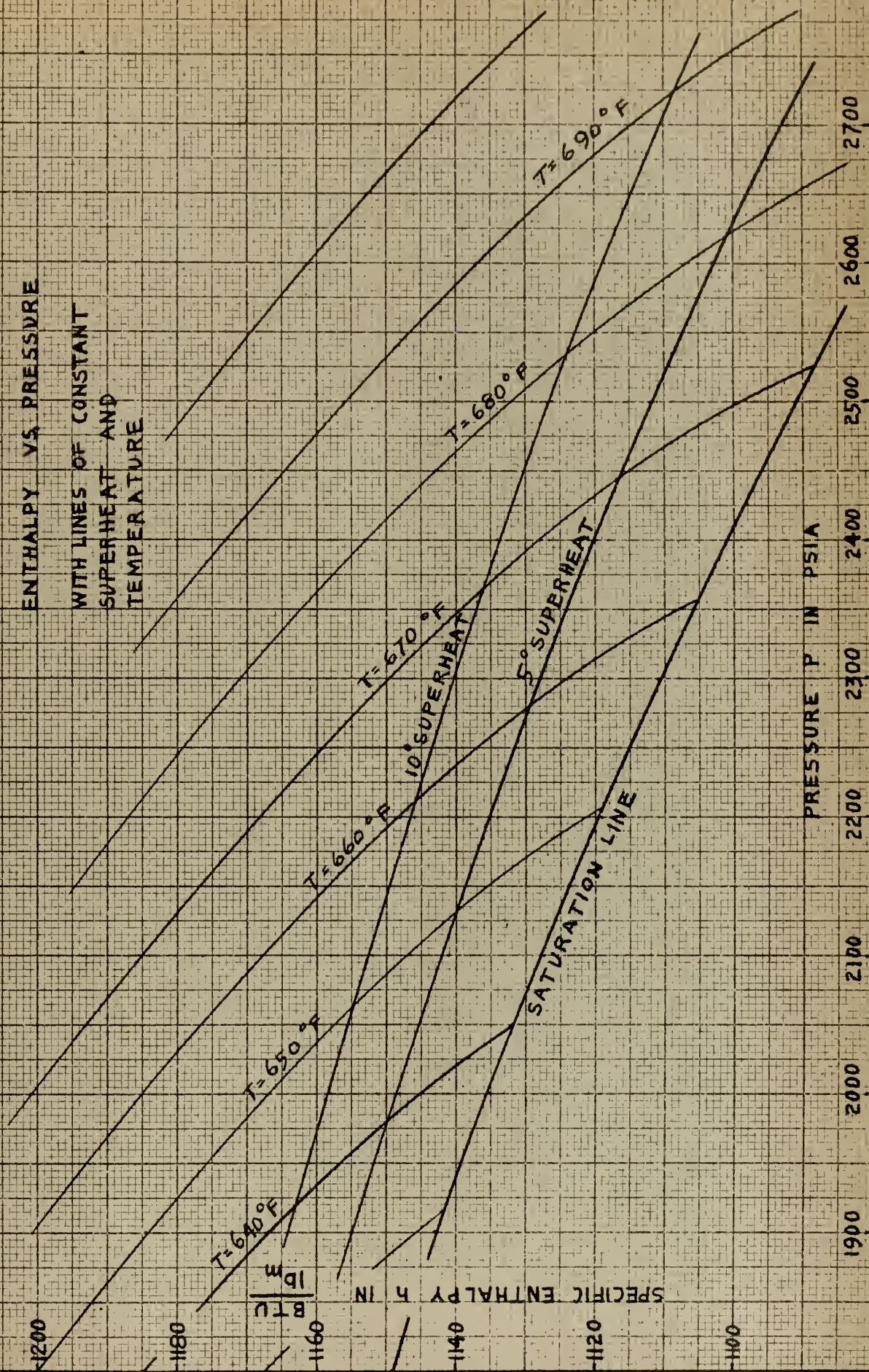


FIGURE 10



TABLE 3

T (°F)	h (BTU/lb)	P (psia)	v (ft <sup>3</sup> /lb)	P v	e (BTU/lb)
630	1186.1	1700	.2558	80.5	1105.6
	1167.7	1800	.2296	76.6	1091.1
	1145.8	1900	.2040	71.8	1074.0
(sat.)	1141.1	1919.3	.1992	70.8	1070.3
640	1185.7	1800	.2407	80.3	1105.4
	1167.0	1900	.2168	76.4	1090.6
	1145.6	2000	.1936	71.7	1073.9
(sat.)	1130.6	2059.7	.1798	68.7	1061.8
650	1167.0	2000	.2058	76.2	1090.8
	1146.3	2100	.1846	71.8	1074.5
	1121.0	2200	.1633	66.4	1054.6
(sat.)	1118.5	2208.2	.1616	66.2	1052.3
660	1167.7	2100	.1962	70.3	1091.4
	1147.3	2200	.1768	72.2	1075.6
	1123.8	2300	.1575	67.3	1056.5
(sat.)	1104.4	2365.4	.1442	63.0	1041.4
670	1150.0	2300	.1702	72.5	1077.5
	1128.2	2400	.1526	67.8	1060.4
	1099.8	2500	.1342	62.2	1037.6
(sat.)	1087.7	2531.8	.1277	59.7	1028.0
680	1132.3	2500	.1484	68.7	1063.6
	1107.1	2600	.1319	63.5	1043.6
	1072.8	2700	.1137	56.8	1016.0
(sat.)	1067.2	2703.1	.1115	56.0	1011.2
690	1156.6	2500	.1594	73.8	1082.8
	1137.3	2600	.1447	69.8	1067.5
	1114.3	2700	.1299	64.8	1049.5
700	1160.6	2600	.1549	74.6	1086.0
	1142.5	2700	.1415	70.7	1071.8





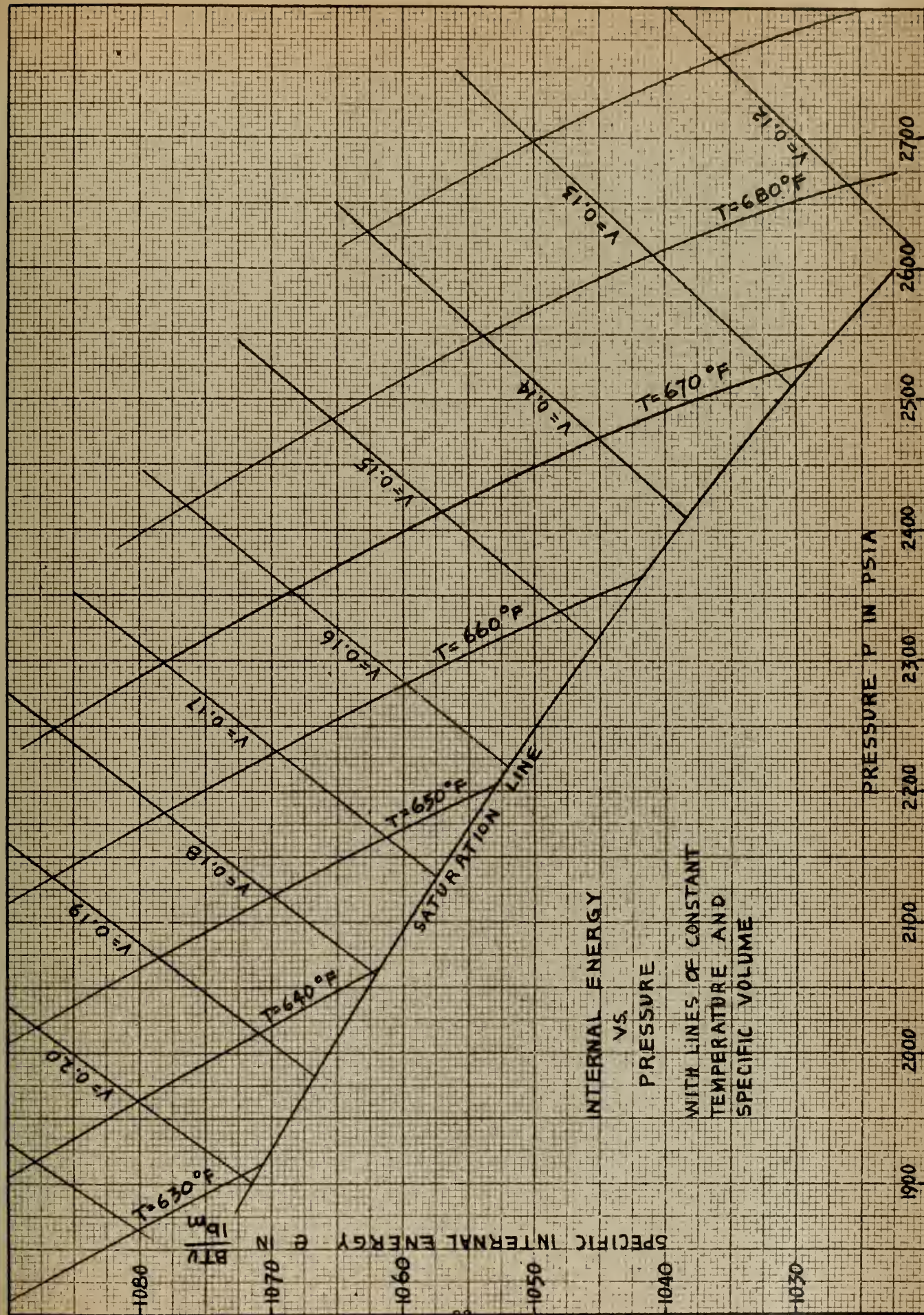


FIGURE 11





TABLE 4

v	e	P	.1176 P	c <sub>14</sub>
.12	1021.0	2620	308.5	712.5
.13	1030.4	2510	295.5	735.0
.14	1038.2	2409	284.0	754.2
.15	1045.4	2312	272.0	773.4
.16	1051.5	2217	261.0	790.5
.17	1056.8	2140	252.0	804.8
.18	1062.0	2057	242.0	820.0
.19	1066.5	1982	233.5	833.0
.20	1070.5	1915	225.5	845.0





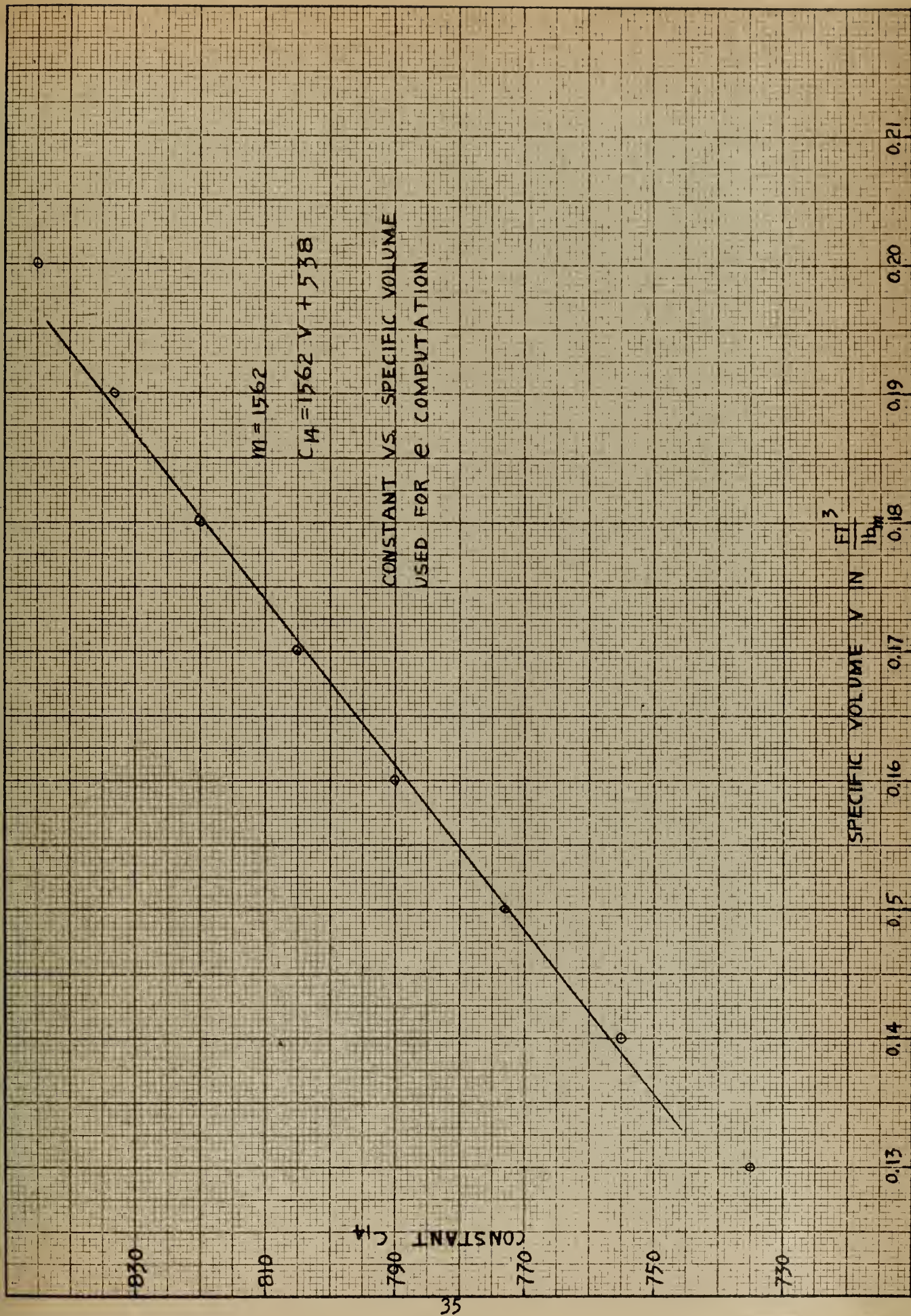


FIGURE 12





additional modification is necessary, making  $e = g(P, v, v^2)$ .

To accomplish this, the expression  $P - 8.51 e = c_{15} v^2 + c_{16} v + c_{17}$  is set up. Substituting actual steam table values at three points ( $P = 1900, 2100, 2300$ ) three simultaneous equations in  $c_{15}$ ,  $c_{16}$ , and  $c_{17}$  result. Solving for these constants and substituting, the final equation for  $P$  is :

$$P = 8.51 e + 52,590 v^2 - 30,700 v - 3161$$

The calculation of an empirical relationship,  $Z = f(P, v)$  follows similar lines. First  $Z$  vs.  $P$  is plotted from the steam tables, showing lines of constant  $v$  (see Fig. 13). The average slope of the constant  $v$  lines is  $1.715 \times 10^{-4}$ , the equation for any one line being  $Z = 1.715 \times 10^{-4} P + c_{18}$ .  $c_{18}$  is determined as a function of  $v$ ,  $c_{18} = 2.943 v - .318$  (see Table 5 and Fig. 14). The expression for  $Z$  as a function of  $P$  and  $v$  is,  $Z = 1.715 \times 10^{-4} P + 2.943 v - .318$ .

Once again a  $v^2$  term is found necessary for desired accuracy, and using the same procedure as before the resulting expression for  $Z$  is:

$$Z = 1.715 \times 10^{-4} P - 9.47 v^2 + 6.048 v - .5693$$



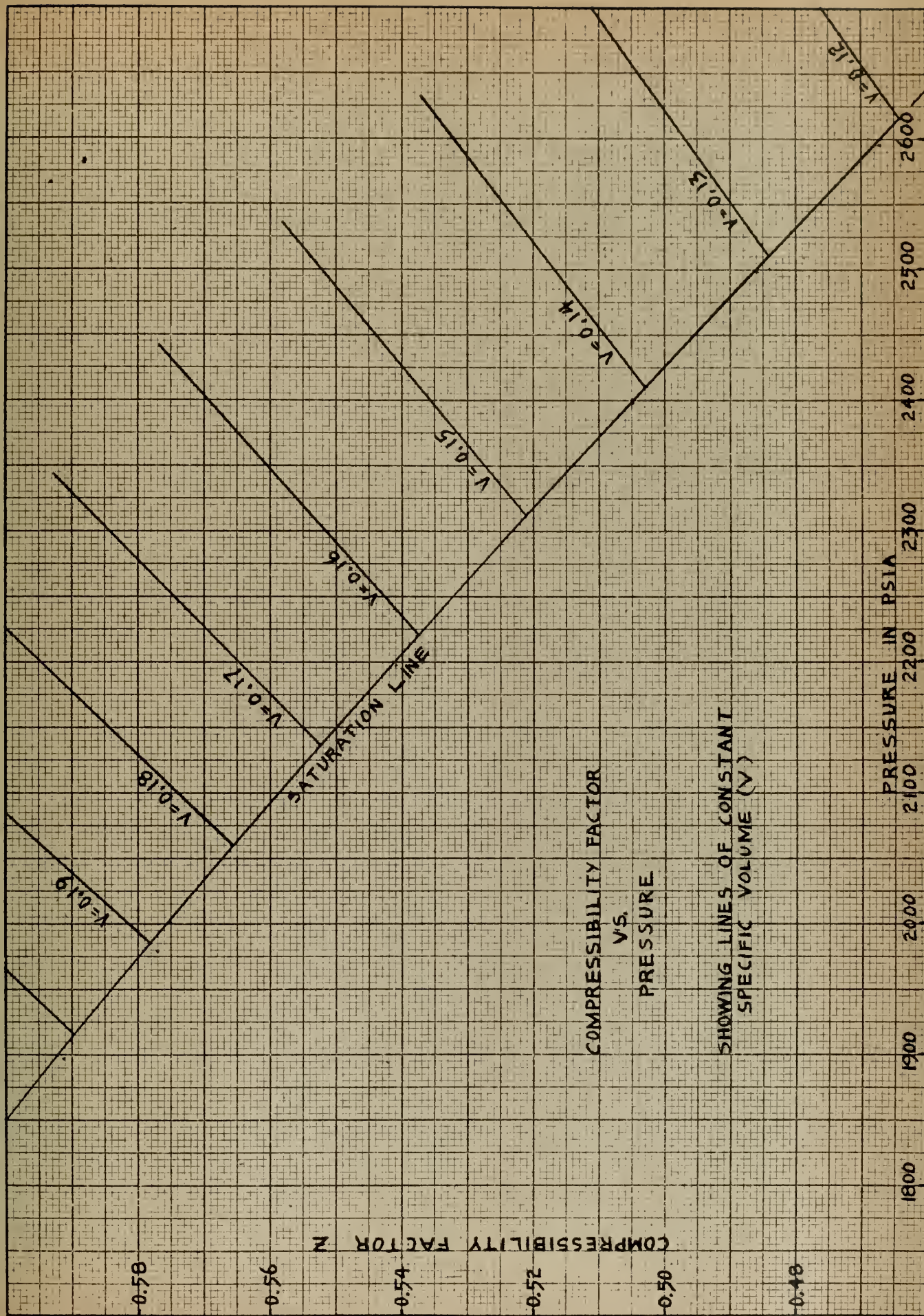


FIGURE 13





TABLE 5

v	Z	P	$1.715 \times 10^{-4} P$	$c_{18}$
.12	.4640	2613	.4475	.0165
.13	.4845	2509	.4300	.0545
.14	.5030	2410	.4130	.0900
.15	.5225	2312	.3960	.1265
.16	.5380	2211	.3790	.1590
.17	.5510	2140	.3670	.1840
.18	.5640	2060	.3530	.2110
.19	.5770	1985	.3405	.2365
.20	.5890	1915	.3280	.2610
.21	.6005	1850	.3170	.2835



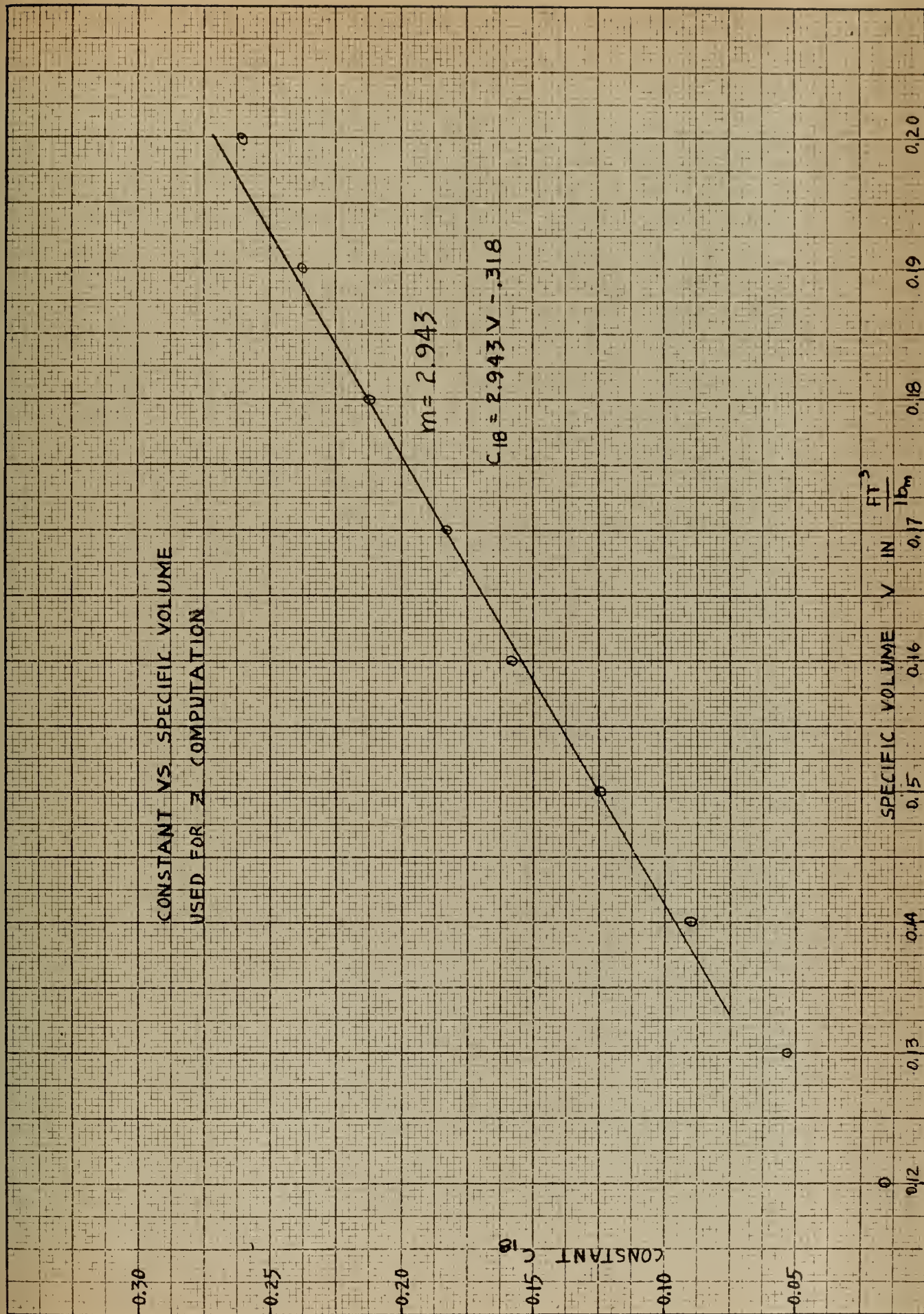


FIGURE 14



## APPENDIX II

### DERIVATION OF MACHINE EQUATIONS

Scaling factors are assigned as follows:

$$\alpha_p = \frac{P_{\max}}{P_{\max}} = \frac{3000}{50} = 60$$

$$\alpha_v = \frac{v_{\max}}{v_{\max}} = \frac{.5}{50} = .01$$

$$\alpha_T = \frac{T_{\max}}{T_{\max}} = \frac{1500}{50} = 30$$

$$\alpha_e = \frac{e_{\max}}{e_{\max}} = \frac{1500}{50} = 30$$

$$\alpha_z = \frac{z_{\max}}{z_{\max}} = \frac{1}{50} = .02$$

$$\alpha_w = \frac{w_{\max}}{w_{\max}} = \frac{50}{50} = 1$$

$$\alpha_q = \frac{q_{\max}}{q_{\max}} = \frac{50}{50} = 1$$

$$\alpha_t = \frac{T}{t} = \frac{1}{1} = 1$$

Conversion of Theoretical Equations to Machine Equations:

$$\#1 \quad w = -\frac{1}{p} \left[ c_{12} P \left( \frac{dv}{dt} \right) dt \right]$$

$$\bar{w} = -\frac{1}{p} \left[ .1851 \left( .1 P \frac{dv}{dt} \right) dt \right] \frac{10 \alpha_p \alpha_v \alpha_t}{\alpha_w \alpha_t}$$

$$\bar{w} = -\frac{1}{p} \left[ 1.111 \left( .1 P \frac{dv}{dt} \right) dt \right]$$





#2

$$e = q + w + e_o$$

$$\bar{e} = \frac{\alpha_q}{\alpha_e} \bar{q} + \frac{\alpha_w}{\alpha_e} \bar{w} + \frac{\alpha_{e_o}}{\alpha_e} \bar{e}_o$$

$$\bar{e} = .0333 \bar{q} + .0333 \bar{w} + \bar{e}_o$$

#3

$$T = \frac{P v}{c_1 Z}$$

$$\left( \frac{.01}{.02} \right) \bar{T} = \frac{\alpha_p \alpha_w}{c_1 \alpha_z \alpha_T} \left[ \frac{.01 P v}{.02 Z} \right]$$

$$\bar{T} = 3.3574 \left[ \frac{.01 P v}{.02 Z} \right]$$

#4

$$P = c_2 e - c_3 v + c_4 v^2 - c_5$$

$$\bar{P} = \frac{\alpha_e c_2}{\alpha_p} \bar{e} - \frac{\alpha_v c_3}{\alpha_p} \bar{v} + 50 \frac{c_4 \alpha_v \alpha_v}{\alpha_p} (.02 \bar{v}^2) - \frac{c_5}{\alpha_p}$$

$$\bar{P} = 4.255 \bar{e} - 5.1167 \bar{v} + 4.3825 (.02 \bar{v}^2) - 52.6833$$

#5

$$Z = c_6 P + c_7 v - c_8 v^2 - c_9$$

$$\bar{Z} = \frac{c_6 \alpha_p}{\alpha_z} \bar{P} + \frac{c_7 \alpha_v}{\alpha_z} \bar{v} - 50 \frac{c_8 \alpha_v \alpha_v}{\alpha_z} (.02 \bar{v}^2) - \frac{c_9}{\alpha_z}$$

$$\bar{Z} = .5145 \bar{P} + 3.024 \bar{v} - 2.3675 (.02 \bar{v}^2) - 28.465$$

#6

$$q = -\frac{1}{p} \left[ c_{10} K (T - T_o) + c_{11} K q \right]$$

$$\bar{q} = -\frac{1}{p} \left[ \frac{c_{10} K \alpha_T}{\alpha_q \alpha_t} (\bar{T} - T_o) + \frac{c_{11} K}{\alpha_t} \bar{q} \right]$$





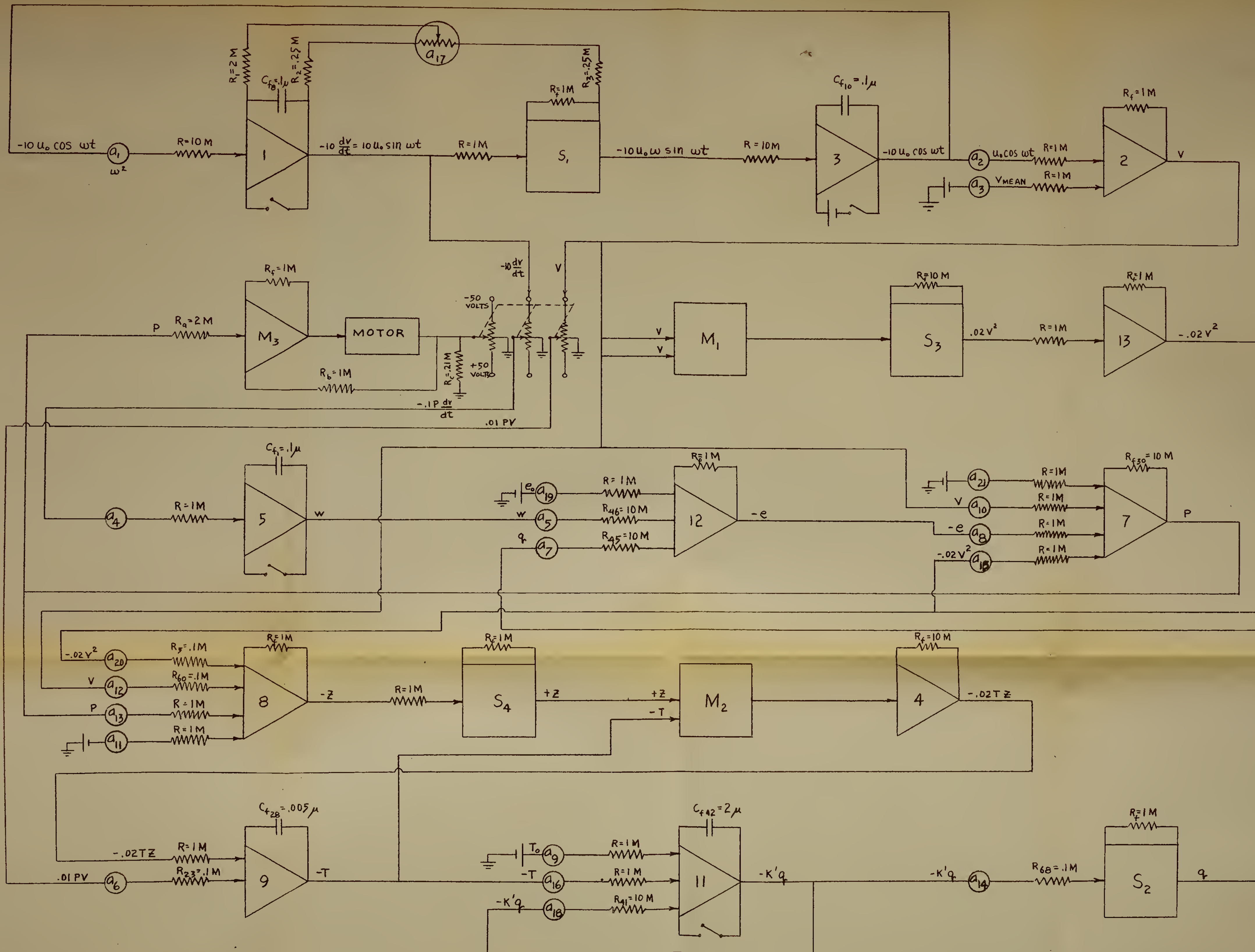
$$\bar{q} = -\frac{1}{p} \left[ .1716 K \bar{T} - .1716 K \bar{T}_0 + .000445 K \bar{q} \right]$$

Calculated potentiometer settings, and components selected:

$a_1$ = D. F. dependent	$a_8$ = .4255	$a_{15}$ = .4383
$a_2$ = " "	$a_9$ = .6864	$a_{16}$ = .6864
$a_3$ = " "	$a_{10}$ = .5117	$a_{17}$ = .5000
$a_4$ = .1111	$a_{11}$ = .6333	$a_{18}$ = .0089
$a_5$ = .3333	$a_{12}$ = .3024	$a_{19} = \frac{\bar{e}_0}{45}$
$a_6$ = .3357	$a_{13}$ = .5145	$a_{20}$ = .2368
$a_7$ = .3333	$a_{14}$ = K	$a_{21}$ = .1182

$R$ = 1 M	$C_{f1}$ = .1 $\mu$ f
$R_{45}$ = 10 M	$C_{f43}$ = 2 $\mu$ f
$R_{46}$ = 10 M	$C_{f8}$ = .1 $\mu$ f
$R_f$ = 1 M	$C_{f10}$ = .1 $\mu$ f
$R_{23}$ = .1 M	$C_{f28}$ = .005 $\mu$ f
$R_{f30}$ = 10 M	
$R_{60}$ = .1 M	
$R_5$ = .1 M	
$R_{41}$ = 10 M	
$R_{68}$ = .1 M	





$M_1, M_2$  FUNCTION MULTIPLIERS  
 $M_3$  SERVO-MULTIPLIER AMPLIFIER  
 $S_1, S_2, S_3, S_4$  SIGN CHANGERS

COMPUTER SCHEMATIC DIAGRAM

FIGURE 15



# APPENDIX III

## HAND SOLUTION OF THEORETICAL EQUATIONS

The first step in obtaining a hand solution consists of combining the six theoretical equations to form two dependent differential equations:

Substituting from equation #2 into equation #4, and then into equation #1 one obtains,

$$\frac{dw}{dt} = -c_{12}c_2 \left[ q + w + e_0 - \frac{c_3}{c_2}v + \frac{c_4}{c_2}v^2 - \frac{c_5}{c_2} \right] \frac{dv}{dt}$$

Since  $v = v_{mean} + u_0 \cos \omega t$

then  $\frac{dv}{dt} = -u_0 \omega \sin \omega t$

and  $\frac{dw}{dt} = u_0 \omega \sin \omega t c_2 c_{12} \left[ q + w - \frac{c_3}{c_2}v + \frac{c_4}{c_2}v^2 + e_0 - \frac{c_5}{c_2} \right]$

Substituting from equations #4 and #5 into equation #3, the resulting expression for T becomes,

$$T = \frac{v \left[ q + w - \frac{c_3}{c_2}v + \frac{c_4}{c_2}v^2 + e_0 - \frac{c_5}{c_2} \right]}{c_1 c_6 \left[ q + w + \left( \frac{c_1}{c_2 c_6} - \frac{c_3}{c_2} \right)v + \left( \frac{c_4}{c_2} - \frac{c_3}{c_2 c_6} \right)v^2 + \left( e_0 - \frac{c_5}{c_2} - \frac{c_9}{c_2 c_6} \right) \right]}$$

It is now convenient to assign values to the driving function, initial conditions, and to evaluate the constants:

$u_0 = .019 \text{ ft}^3/\text{lb}$	$c_2 = 8.51$	$c_7 = 6.048$
$\omega = .0418 \text{ rad/sec}$	$c_3 = 3.07 \times 10^4$	$c_8 = 9.47$
$v_{mean} = .172 \text{ ft}^3/\text{lb}$	$c_4 = 5.259 \times 10^4$	$c_9 = .5693$
$e_0 = 1066 \text{ BTU/lb}$	$c_5 = 3161$	$c_{12} = .1853$
$c_1 = .5957$	$c_6 = 1.714 \times 10^{-4}$	





Evaluating,

$$\frac{dw}{dt} = 1.253 \times 10^{-3} \sin .0418 t [q + w - 3610 v + 6180 v^2 + 694]$$

$$T = \frac{9800 v [q + w - 3610 v + 6180 v^2 + 694]}{[q + w + 540 v - 310 v^2 + 304]}$$

Equation #6 is,

$$\frac{dq}{dt} = -C_{10} K T + C_{10} K T_0 - C_{11} K q$$

Arbitrarily assigning a value to  $k$ , evaluating constants, and substituting the already derived expression for  $T$  into equation #6,

$$K = .9254$$

$$C_{10} = 5.72 \times 10^{-3}$$

$$C_{11} = 4.45 \times 10^{-4}$$

$$T_0 = 1094.5 \text{ } ^\circ R$$

$$\frac{dq}{dt} = -51.8 v \frac{[q + w - 3610 v + 6180 v^2 + 694]}{[q + w + 540 v - 310 v^2 + 304]} - 4.12 \times 10^{-4} q + 5.770$$

The two resulting dependent first order differential equations become,

$$\frac{dq}{dt} = K_1 \frac{[q + w + K_2]}{[q + w + K_3]} - 4.12 \times 10^{-4} q + 5.770$$

$$\frac{dw}{dt} = K_4 [q + w + K_2]$$

where  $K_1, K_2, K_3, K_4$  are tabulated values of  $v$ , the driving function (see Table 6).



TABLE 6

Time	$u_0 \cos \omega t$	$v$	$K_1$	$K_2$	$K_3$	$K_4$
0	.0190	.1910	-9.90	230.5	395.7	0
5	.0186	.1906	-9.88	231.0	395.5	$2.61 \times 10^{-4}$
10	.0174	.1893	-9.82	232.0	395.1	5.10 "
15	.0154	.1873	-9.71	235.0	394.3	7.38 "
20	.0127	.1847	-9.58	239.0	393.1	9.33 "
25	.0095	.1815	-9.41	242.5	391.8	10.87 "
30	.0059	.1779	-9.24	247.5	390.3	11.90 "
35	.0020	.1740	-9.02	253.0	388.6	12.47 "
40	-.0020	.1700	-8.82	259.5	386.8	12.47 "
45	-.0059	.1661	-8.62	264.5	385.2	11.90 "
50	-.0095	.1615	-8.37	272.3	383.1	10.87 "
55	-.0127	.1593	-8.26	276.0	382.1	9.33 "
60	-.0154	.1567	-8.13	281.0	381.0	7.38 "
65	-.0174	.1547	-8.02	283.7	380.1	5.10 "
70	-.0186	.1534	-7.95	285.0	379.6	2.61 "
75	-.0190	.1530	-7.94	286.5	379.5	0
80	-.0186	.1534	-7.95	285.0	379.6	-2.61 "
85	-.0174	.1547	-8.02	283.7	380.1	-5.10 "
90	-.0154	.1567	-8.13	281.0	381.0	-7.38 "
95	-.0127	.1593	-8.26	276.0	382.1	-9.33 "
100	-.0095	.1615	-8.37	272.3	383.1	-10.87 "



The next step consists of numerically integrating the above equations to obtain point-by-point values of  $q$ ,  $\frac{dq}{dt}$ ,  $w$ , and  $\frac{dw}{dt}$ . The Heun Method of numerical integration is used, the general form

being:

$$\dot{q} = f(w, q, v)$$

$$\dot{w} = g(w, q, v)$$

$$q_i^{(n)} = q_{i-1} + \frac{h}{2} (\dot{q}_{i-1} + \dot{q}_i^{(n-1)})$$

where

$$q_i^{(n)} = q_{i-1} + h (\dot{q}_{i-1})$$

$$w_i^{(n)} = w_{i-1} + \frac{h}{2} (\dot{w}_{i-1} + \dot{w}_i^{(n-1)})$$

where

$$w_i^{(n)} = w_{i-1} + h (\dot{w}_{i-1})$$

$h$  is the interval between points and is selected as 5 seconds.

Table 7 lists the resulting values for  $q$ ,  $\dot{q}$ ,  $w$ , and  $\dot{w}$  obtained over a time of 100 seconds (21 points).

Next, the resulting values of  $q$  and  $w$  are substituted back into the original theoretical equations, resulting in point-by-point values for the various properties throughout the run. These values are tabulated (see Table 8), and are plotted as a function of time in Fig. 4, Chapter IV.





TABLE 7  
HAND SOLUTION (K = .9265)

i	t	$q_i$	$\dot{q}_i$	$w_i$	$\dot{w}_i$
0	0	0	0	0	0
1	5	-.0273	-.0110	.1509	.0604
2	10	-.1083	-.0215	.6011	.1197
3	15	-.3410	-.0716	1.3431	.1772
4	20	-.8431	-.1292	2.3614	.2302
5	25	-1.5479	-.1527	3.6260	.2757
6	30	-2.4188	-.1957	5.0948	.3119
7	35	-3.4896	-.2327	6.7173	.3372
8	40	-4.7612	-.2760	8.4311	.3483
9	45	-6.1402	-.2756	10.1536	.3407
10	50	-7.5859	-.3026	11.8070	.3206
11	55	-9.1078	-.3062	13.3039	.2781
12	60	-10.6548	-.3126	14.5556	.2226
13	65	-12.1476	-.2845	15.4969	.1539
14	70	-13.4683	-.2438	16.0765	.0779
15	75	-14.6571	-.2317	16.2714	0
16	80	-15.6849	-.1794	16.0843	-.0748
17	85	-16.5174	-.1536	15.5423	-.1420
18	90	-17.1731	-.1087	14.6944	-.1972
19	95	-17.5063	-.0246	13.6080	-.2374
20	100	-17.4614	.0426	12.3475	-.2659



TABLE 8  
PROPERTY VALUES FROM HAND SOLUTION

t	e	v	P	Z	T
0	1066.0	.1910	1966.9	.5774	1092.1
5	1066.12	.1906	1969.7	.5774	1091.3
10	1066.49	.1893	1986.4	.5773	1093.4
15	1067.0	.1873	2015.4	.5766	1098.9
20	1067.52	.1847	2047.0	.5760	1101.9
25	1068.08	.1815	2086.9	.5747	1106.5
30	1068.68	.1779	2134.2	.5734	1111.4
35	1069.23	.1740	2190.1	.5718	1118.8
40	1069.67	.1700	2243.0	.5699	1123.1
45	1070.01	.1661	2297.3	.5679	1127.9
50	1070.22	.1615	2361.5	.5653	1132.6
55	1070.20	.1593	2391.9	.5638	1134.3
60	1069.90	.1567	2427.1	.5616	1137.0
65	1069.35	.1547	2447.0	.5597	1135.4
70	1068.61	.1534	2459.6	.5578	1135.4
75	1067.61	.1530	2458.1	.5560	1135.5
80	1066.40	.1534	2440.8	.5546	1133.2
85	1065.02	.1547	2390.1	.5499	1128.6
90	1063.29	.1567	2370.9	.5520	1129.9
95	1062.10	.1593	2323.0	.5520	1125.5
100	1060.69	.1615	2282.1	.5517	1121.6



APPENDIX IV  
ACTUAL TANK TRANSIENT DATA

Run #2247

$m_0 = 169.06 \text{ lb.}$

Time	Pressure	Level	Volume	Spec. Vol.
0	2002	32.2	31.7	.1875
5	2012	32.4	31.6	.1867
10	2042	33.2	31.2	.1843
15	2094	34.6	30.4	.1797
20	2168	36.7	29.1	.1720
25	2233	39.7	27.3	.1612
30	2280	41.8	26.1	.1542
35	2305	43.1	25.4	.1500
40	2316	43.7	25.1	.1485

Run #2240

$m_0 = 167.46 \text{ lb.}$

0	2002	32.8	31.4	.1875
5	2007	33.0	31.3	.1870
10	2026	33.5	31.0	.1850
15	2047	34.1	30.6	.1827
20	2071	34.9	30.2	.1803
25	2091	35.6	29.7	.1773
30	2104	36.3	29.5	.1760
35	2112	36.8	29.0	.1731
40	2112	37.0	28.9	.1726





Run #2229

 $m_o = 167.13 \text{ lb.}$ 

Time	Pressure	Level	Volume	Spec.Vol.
0	1992	32.5	31.5	.1885
10	2007	33.0	31.3	.1873
20	2033	33.9	30.8	.1843
30	2070	35.2	30.1	.1800
40	2117	36.8	29.0	.1735
50	2170	38.6	28.0	.1675
60	2220	40.4	27.0	.1615
70	2264	41.8	26.1	.1560
80	2295	42.7	25.7	.1537

Run #2128

 $m_o = 169.05 \text{ lb.}$ 

0	2000	32.3	31.7	.1875
10	2012	32.7	31.5	.1861
20	2037	33.4	31.0	.1832
30	2072	34.5	30.4	.1796
40	2114	36.0	29.5	.1743
50	2162	37.8	28.5	.1684
60	2211	39.5	27.4	.1620
70	2244	41.0	26.6	.1572
80	2288	42.0	26.0	.1537
90	2299	42.6	25.7	.1520
100	2299	42.7	25.6	.1514



Run #2113

 $m_o = 172.7 \text{ lb.}$ 

Time	Pressure	Level	Volume	Spec.Vol.
0	2000	31.2	32.4	.1878
2.5	2002	31.4	32.3	.1870
5	2019	31.8	32.0	.1854
7.5	2054	32.4	31.6	.1830
10	2090	33.3	31.0	.1795
12.5	2124	34.3	30.5	.1765
15	2155	35.3	29.9	.1730
17.5	2172	36.2	29.4	.1703
20	2182	36.9	29.0	.1680
22.5	2186	37.3	28.7	.1662
25	2187	37.6	28.5	.1650
27.5	2187	37.9	28.4	.1645
30	2187	38.0	28.3	.1640

Run #1101

 $m_o = 169.5 \text{ lb.}$ 

0	1990	31.6	32.1	.1892
2.5	1995	31.8	32.0	.1888
5	2009	32.3	31.7	.1870
7.5	2039	32.8	31.4	.1854
10	2066	33.5	31.0	.1830
12.5	2085	34.4	30.4	.1793
15	2097	34.9	30.1	.1775
17.5	2102	35.3	29.9	.1765
20	2102	35.5	29.8	.1760



Run #2255

 $m_o = 175.0 \text{ lb.}$ 

Time	Pressure	Level	Volume	Spec. Vol.
0	1995	30.0	33.0	.1885
2.5	2002	30.1	33.0	.1885
5	2011	30.3	32.9	.1880
7.5	2032	30.6	32.7	.1870
10	2043	31.1	32.4	.1850
12.5	2055	31.7	32.0	.1828
15	2094	32.5	31.6	.1805
17.5	2121	33.3	31.1	.1775
20	2134	34.0	30.7	.1755
22.5	2143	34.6	30.3	.1730
25	2146	35.0	30.0	.1715
27.5	2147	35.3	29.9	.1710
30	2147	35.5	29.8	.1703

Run #1506

 $m_o = 167.7 \text{ lb.}$ 

0	1952	30.8	32.6	.1944
5	1958	30.9	32.5	.1940
10	1988	31.7	32.0	.1908
15	2032	33.0	31.3	.1867
20	2082	34.4	30.4	.1812
25	2130	35.7	29.7	.1770
30	2174	37.1	28.8	.1718
35	2217	38.5	28.0	.1670
40	2238	39.7	27.3	.1629
45	2241	40.0	27.1	.1616





Run #1556

 $m_0 = 159.7 \text{ lb.}$ 

Time	Pressure	Level	Volume	Spec. Vol.
0	1893	31.2	32.4	.2030
5	1894	31.3	32.3	.2022
10	1923	32.0	31.9	.2000
15	1960	33.0	31.3	.1962
20	1998	34.2	30.5	.1912
25	2034	35.4	29.8	.1868
30	2063	36.5	29.3	.1837
35	2086	37.3	28.7	.1798
40	2101	38.0	28.3	.1774
45	2114	38.7	28.1	.1761
50	2122	39.1	27.5	.1723
55	2122	39.4	27.4	.1718

Run #2010

 $m_0 = 164.6 \text{ lb.}$ 

0	1930	31.0	32.5	.1975
5	1933	31.0	32.5	.1975
10	1942	31.1	32.5	.1975
15	1962	31.5	32.1	.1951
20	1988	32.3	31.7	.1927
25	2021	33.2	31.2	.1898
30	2057	34.4	30.5	.1855
35	2094	35.4	29.8	.1812
40	2124	36.4	29.3	.1782
45	2146	37.0	28.9	.1757
50	2159	37.6	28.6	.1740
55	2162	37.9	28.4	.1727



Run #2023

 $m_o = 166.6 \text{ lb.}$ 

Time	Pressure	Level	Volume	Spec.Vol.
0	1946	31.0	32.5	.1952
5	1949	31.0	32.5	.1952
10	1962	31.2	32.3	.1940
15	1982	31.7	32.1	.1928
20	2008	32.5	31.6	.1899
25	2040	33.4	31.0	.1862
30	2074	34.5	30.4	.1827
35	2111	35.7	29.7	.1784
40	2144	36.5	29.2	.1753
45	2168	37.2	28.8	.1730
50	2180	37.7	28.5	.1711
55	2186	38.1	28.3	.1700
60	2188	38.3	28.2	.1694

Run #1630

 $m_o = 198.3 \text{ lb.}$ 

0	1938	20.0	39.0	.1967
10	1952	20.6	38.6	.1948
20	1982	21.5	38.1	.1920
30	2022	22.8	37.3	.1880
40	2074	24.8	36.1	.1830
50	2132	26.7	35.0	.1775
60	2184	27.8	34.4	.1722
70	2224	29.8	33.2	.1670
80	2252	31.4	32.2	.1623
90	2262	32.6	31.5	.1589



Run #1911

m<sub>0</sub> = 184.7 lb.

Time	Pressure	Level	Volume	Spec.Vol.
0	1910	23.2	37.1	.2007
2.5	1920	23.6	36.8	.2004
5	1935	23.8	36.7	.1993
7.5	1958	24.2	36.6	.1974
10	1990	25.4	35.8	.1950
12.5	2027	26.0	35.4	.1914
15	2072	27.5	34.5	.1872
17.5	2117	28.8	33.8	.1830
20	2161	30.0	33.1	.1788
22.5	2207	31.8	32.0	.1737
25	2252	33.0	31.3	.1690
27.5	2287	34.5	30.4	.1645
30	2312	35.7	29.7	.1607
32.5	2323	36.7	29.1	.1572
35	2327	37.3	28.7	.1553
37.5	2327	37.5	28.6	.1548



Run #1658

 $m_o$  - 134.1 lb.

Time	Pressure	Level	Volume	Spec. Vol.
0	1972	26.2	35.3	.1918
10	1972	26.4	35.2	.1916
20	1982	26.5	35.1	.1906
30	2002	27.4	34.5	.1877
40	2045	28.9	33.7	.1830
50	2092	30.8	32.6	.1775
60	2147	32.5	31.6	.1713
70	2200	34.6	30.4	.1651
80	2249	36.3	29.3	.1591
90	2278	37.7	28.5	.1544
95	2282	38.2	28.2	.1532





Run #2248

 $m_0 = 158.3 \text{ lb.}$ 

Time	Pressure	Level	Volume	Spec.Vol.
0	1903	31.8	31.9	.2017
2.5	1903	31.8	31.9	.2017
5	1907	31.8	31.9	.2017
7.5	1912	32.0	31.8	.2008
10	1923	32.3	31.7	.2000
12.5	1948	32.8	31.4	.1982
15	1987	33.6	31.0	.1958
17.5	2033	34.6	30.3	.1912
20	2084	35.8	29.6	.1869
22.5	2125	37.0	28.9	.1825
25	2150	38.0	28.3	.1787
27.5	2162	38.6	27.8	.1755
30	2164	39.2	27.6	.1742
32.5	2164	39.4	27.5	.1735
35	2164	39.5	27.4	.1730



Run #2302

 $m_o = 162.5 \text{ lb.}$ 

Time	Pressure	Level	Volume	Spec.Vol.
0	1888	30.0	33.0	.2032
10	1891	30.2	32.9	.2025
20	1902	30.5	32.8	.2020
30	1918	31.0	32.5	.2000
40	1935	31.6	32.1	.1975
50	1955	32.3	31.7	.1952
60	1975	33.1	31.2	.1921
70	1996	34.0	30.7	.1890
80	2017	34.8	30.2	.1860
90	2038	35.5	29.8	.1835
100	2054	36.1	29.4	.1810
110	2062	36.4	29.3	.1804
120	2062	36.5	29.2	.1798



Run #2045

 $m_o = 167.0 \text{ lb.}$ 

Time	Pressure	Level	Volume	Spec.Vol.
0	1982	32.0	31.8	.1904
5	1990	32.5	31.6	.1894
10	2005	32.8	31.4	.1880
15	2025	33.5	31.0	.1856
20	2054	34.5	30.4	.1823
25	2091	35.5	29.8	.1785
30	2130	36.6	29.1	.1746
35	2166	37.5	28.6	.1710
40	2197	38.5	28.0	.1674
45	2227	39.5	27.4	.1640
50	2252	40.5	26.9	.1610
55	2275	41.3	26.5	.1584
60	2290	41.9	26.1	.1562
65	2295	42.1	26.0	.1548
70	2295	42.5	25.7	.1539





Run #2039

W<sub>0</sub> = 165.5 lb.

Time	Pressure	Level	Volume	Spec. Vol.
0	1981	32.7	31.5	.1905
2.5	1981	32.7	31.4	.1902
5	1986	33.0	31.3	.1896
7.5	1995	33.2	31.2	.1888
10	2008	33.6	31.0	.1874
12.5	2025	34.1	30.6	.1854
15	2045	34.7	30.3	.1832
17.5	2068	35.4	29.8	.1802
20	2098	36.1	29.4	.1770
22.5	2137	37.8	28.5	.1734
25	2177	38.2	28.2	.1698
27.5	2217	39.2	27.6	.1662
30	2252	40.3	27.0	.1626
32.5	2286	41.2	26.5	.1590
35	2312	42.4	25.8	.1560
37.5	2322	43.1	25.4	.1540











AG 24 63

13099

Thesis  
B725

23030

Bosley

Simulation of steam  
pressurizing tank  
transients by analog  
computer.

AG 24 63

13099

Th  
B7

Thesis  
B725

23080

Bosley

Simulation of steam  
pressurizing tank transients by  
analog computer.



thesB725

Simulation of steam pressurizing tank tr



3 2768 002 07324 9

DUDLEY KNOX LIBRARY